THESIS

INTERACTION BETWEEN MEMBRANE & PROTEIN PROPERTIES ON FLUX DECLINE

DURING STERILE MICROFILTRATION

Submitted by

Hailey Cutler

Graduate Degree Program in Bioengineering

In partial fulfillment of the requirements

For the Degree of Master of Science

Colorado State University

Fort Collins, Colorado

Summer 2010

COLORADO STATE UNIVERSITY

July 12, 2010

WE HEREBY RECOMMEND THAT THE THESIS PREPARED UNDER OUR

SUPERVISION BY HAILEY CUTLER ENTITLED <u>INTERACTION BETWEEN</u>

<u>MEMBRANE AND PROTEIN PROPERTIES ON FLUX DECLINE DURING STERILE</u>

<u>MICROFILTRATION</u> BE ACCEPTED AS FULFILLING IN PART REQUIREMENTS FOR

THE DEGREE OF MASTER OF SCIENCE.

<u>Committee on Graduate Work</u>

_____
Matt J. Kipper

_____
S. Karan Venayayamoorthy

_____
Advisor: S. Ranil Wickramasinghe

_____
Director: Stuart A. Tobet

ABSTRACT OF THESIS

INTERACTION BETWEEN MEMBRANE & PROTEIN PROPERTIES ON FLUX DECLINE

DURING STERILE MICROFILTRATION

Microfiltration is widely used in industry to filter out particulate matter that contaminates or slows down the performance of the membrane. In the biopharmaceutical industry in particular, bacteria, microorganisms and viruses are filtered out using sterile microfiltration. Numerous studies have been conducted to further the understanding of flux decline due to protein fouling. Many times the operating conditions, the type of membrane and type of protein all interact to have an effect on protein fouling and flux decline.

Normal-flow microfiltration experiments were conducted using uncoated polytetrafluoroethylene (PTFE) and polyvinylidene fluoride (PVDF) membranes, and PTFE and PVDF membranes coated with polyvinyl alcohol (PVA). Feed streams consisted of lysozyme, β-lactoglobulin and ovalbumin. The pH values of the solution were set at the isoelectric point of each of the proteins (11.0, 5.8, and 4.7 respectively). The experiments were operated with a feed pressure of 2 or 10 psi. Each of the proteins was tested at 0.1 and 2 g/L with uncoated PTFE. No flux decline was seen using 0.1 g/L, so 2 g/L was focused on for PVA coated PTFE, PVA coated PVDF and uncoated PVDF membranes. Protein fouling of the membrane was investigated by determining the variation of permeate flux versus filtrate volume and by analysis of Attenuated Total Reflection-Fourier Transform Infrared (ATR-FTIR) spectra and Field Emission Scanning Electron Microscopy (FESEM) images of unfouled membranes and membranes after microfiltration.

Results indicate that the greatest amount of fouling occurs with ovalbumin. The order of most to least fouling was found to be ovalbumin> β-lactoglobulin>lysozyme. Fouling was more severe at the higher protein concentration (2 g/L) and feed pressure (10 psi) and seen only when filtering the solution through uncoated and PVA coated PTFE. Flux decline under these conditions was analyzed using classical pore blockage models. In general, flux decline was found to be caused by complete pore blocking. In the case of ovalbumin filtered through PVA coated PTFE, the flux decline was first caused by pore blockage and then later transitioned to cake filtration.

The proteins which showed significant fouling conditions were looked at more closely by pre-filtering the protein solution. The goal of pre-filtration was to decrease any protein aggregates present in solution. This pre-filtration step was conducted with 0.2, 0.45 and 1 μm diameter pore sizes. The flux decline when pre-filtering the feed solution with 1 μm pores was equivalent to the filtration experiments without pre-filtration. The only significant decrease in flux was present when pre-filtering with the 1μm pores.

Additional experiments were conducted using hemoglobin (Hb) at 2 g/L and 10 psi operating conditions. Previous literature had shown that using 1 μm pre-filtration, there was severe flux decline for uncoated and PVA coated PTFE. To follow up on these experiments, Hb was pre-filtered using 0.2 and 0.45 μm pre-filtration membranes and then filtered through uncoated and PVA coated PTFE. These experiments resulted in no flux decline. The Hb experiments verified the results from the ovalbumin and β-lactoglobulin experiments.

All together, these results indicate that there is an interaction among membrane properties, protein properties, operating conditions and pre-filtration characteristics that determine whether fouling occurs and to what extent.

Hailey Jo Elizabeth Cutler
Graduate Degree Program in Bioengineering
Colorado State University
Fort Collins, CO 80523
Summer 2010

ACKNOWLEDGEMENTS

TABLE OF CONTENTS

TABLE OF FIGURES AND TABLES

CHAPTER 1. INTRODUCTION

Microfiltration is one of many types of different filtrations and is used to filter out some of the largest particulates in solution. It has been used to a great extent in biotechnology and pharmaceutical industries [1]. It is used for filtration of therapeutic proteins, clarification and sterilization of many biological solutions and beverages, fermentation broths, and plasma collection from whole blood [1, 2]. However, the biggest problem with microfiltration is protein fouling. Protein fouling can be initiated from interactions between the membrane and the protein [1] and causes a significant reduction in membrane performance and could lead to loss of valuable product [2]. This fouling leads to irreversible modification to the surface of the membrane that causes flux decline and changes in membrane rejection [1]. In industry the membranes need to be cleaned or replaced to have the optimum membrane filtration properties.

While many filtered solutions will produce a decrease in flux and transmission, biological foulants such as proteins have been known to be especially difficult. Proteins can absorb to smooth surfaces or they can deposit on the membrane via convection [3]. Since there are multiple mechanisms, it can be difficult to characterize the method of fouling. Also proteins can denature or aggregate which adds more complexity in the method of deposition [3].

The purpose of this research is to determine the reasons for permeate flux decline during microfiltration. We hypothesize that this occurrence of reduction in flux is due to the different properties of membranes, the protein properties, and operating conditions. Each of these three main sources has multiple sub-properties that all can affect the flux decline. When looking at membranes they have different pore morphology and surface chemistry that can play a role in

flux decline. The type of protein has a significant effect on flux decline based on the size, conformation and isoelectric point. In this case each of the proteins is similar in size, each is globular, and all solutions are at the protein's isoelectric point. Lastly, the different operating conditions for the experiments have an effect. Depending on the feed pressure, pH of the solution and concentration of the solution, these all can be responsible for a significant flux decline.

For this project we focus on three different proteins; lysozyme, β-lactoglobulin, and ovalbumin. Each of these are commonly used. The two types of membranes used for the experiments were polytetrafluoroethylene (PTFE) provided by W.L. Gore & Associates (Newark, MD) and polyvinylidene fluoride (PVDF) acquired from Millipore (Bedford, MA). These both have a nominal pore size of 0.45 μm. For PTFE and PVDF, they each had two surface chemistries investigated; hydrophobic (uncoated) and hydrophilic (PVA coated). Two different protein concentrations (0.1 & 2 g/L) and two pressures (2 & 10 psi) were used. The isoelectric point of each of the three proteins was used and the experiments were conducted at room temperature. Pre-filtration was also conducted using three membranes with varying pore sizes. Nylaflo^TM with a nominal pore size of 0.2 μm was supplied by Pall (Ann Arbor, MI), uncoated PTFE membrane with a nominal pore size of 0.45 μm was supplied by W.L. Gore & Associates (Newark, DE) and Whatman Grade No. 1 Filter Paper with approximately 1μm nominal pore size. The UV spectrophotometer was utilized to determine protein transmission for each experiment. Two different surface characterization methods were used: ATR Attenuated Total Reflection-Fourier Transform Infrared (ATR-FTIR) spectra and Field Emission Scanning Electron Microscopy (FESEM) which helped to study the surfaces of cleaned and fouled membranes. Also the fouling mechanism prediction models were applied to the data to determine which fouling mechanism caused the permeate flux to decline.

CHAPTER 2. BACKGROUND AND THEORY

2.1 MICROFILTRATION MEMBRANES

(i) Membrane Materials

Membranes are used for many different applications and are known as a selective barrier separating two phases. There are biological or synthetic membranes and both of these can be narrowed down into smaller categories [4]. In particular for microfiltration, synthetic membranes are used in industry and laboratory settings for a number of filtration purposes. Microfiltration membranes are normally made of organic materials which are polymers or inorganic materials which consist of ceramic, metal or glass [4]. There are four different methods used to produce membranes from polymers. These are sintering, stretching, track-etching and phase inversion [4-6]. Numerous synthetic polymeric membranes can be prepared by these methods and these resulting membranes can be divided into two classes; hydrophobic and hydrophilic. Hydrophobic membranes will not be wetted by water and it is difficult to get water to flow through the membrane under normal pressures [4]. This gives hydrophobic membranes a predisposition to fouling since it is difficult to push water through the membrane. The majority of membranes in this classification are polypropylene (PP), polytetrafluoroethylene (PTFE), poly(vinylidene fluoride) (PVDF), and polyethylene (PE) [4]. Membranes that have a hydrophilic surface are useful to provide better flow through the membrane. The most common hydrophilic membranes made of polymers are cellulose esters, polycarbonate (PC), polysulfone/poly(ether sulfone), polyimide/poly(ether imide), polyamide (PA), and polyetheretherketone (PEEK) [4].

2.2 MICROFILTRATION

There are many different types of filtration which have been named based on size of the particles that can be effectively separated. In general there are four main types of filtration; microfiltration, ultrafiltration, nanofiltration, and reverse osmosis [7]. While microfiltration can filter larger particles in the 0.1-10 µm range, ultrafiltration, nanofiltration and reverse osmosis operate on a much smaller size scales and each are able to filter smaller solutes respectively [4]. Since the pore size for microfiltration membranes is larger, the permeate flux is also larger than the other types of filtration.

Microfiltration uses pressure drop as the driving force for the process. The operating pressure typically ranges from 1 to 50 psi [4]. This driving force is able to initiate the filtration process. The liquid and smaller solutes are able to pass through the membrane producing a permeate stream while particles larger than the membrane pore diameter will be retained by the membrane such as bacteria, microorganisms and viruses [5].

The process of using microfiltration can be implemented in two different arrangements based on the operating requirements. These two arrangements are called dead end or normal flow filtration and tangential flow or cross flow filtration [4-7].

Dead end filtration is set up so that the feed solution flows perpendicularly through the membrane and the permeate product is collected from the bottom as seen in Figure 1. In particular, sterile filtration is operated in dead end filtration mode. The solutes within the solution begin to build up on the surface of the membrane if they cannot pass through the pores [4]. This leads to a layer of retained particulates to form on top of the membrane which increases the resistance to filtration. This in turn results in a decrease in permeate flux when the pressure drop is held constant. If the permeate flux is held constant, however, this results in the pressure drop increasing. Although this can be a disadvantage, dead end filtration is useful for processing large

amounts solution in a timely manner. However, the membrane may need to be replaced often due to buildup of foulants.

Tangential flow filtration is arranged so that the feed solution flows parallel to the membrane surface and the permeate product is collected out the bottom shown in Figure 1. Particles can also form a cake layer on the membrane surface, but this is not as critical because the liquid flowing across the membrane exerts shear on the particles so that the cake layer cannot continue to grow over time [4]. In this configuration, high fluxes can be maintained. This configuration can be set up so that the retentate or the outlet stream can be recycled to produce a higher recovery in the permeate.

While both dead end and tangential flow filtration can be used to successfully filter bacteria and microorganisms, they have advantages and disadvantages to each. Since the solution for dead end filtration is fed perpendicularly to the membrane, this initiates a concentration gradient to develop near the surface of the membrane and increases fouling and decreases permeate flux [4]. For tangential flow filtration this buildup is effectively controlled by the shear from the flowing liquid placed on the particles. Although tangential flow filtration is better at limiting the amount of cake layer build up, it does not have as high of a product yield as dead end filtration [4]. This is due to the stream carrying some of the fluid out to the retentate.

Microfiltration is used in many different industries and for a wide range of purposes. While this does not include all of the diverse applications, it gives an overview of the variety of functions microfiltration has. Microfiltration is used for cold sterilization of beverages and pharmaceuticals, cell harvesting, waste water treatment, clarification of beverages, plasmapheresis, and continuous fermentation [4]. Microfiltration membranes set up in dead end filtration mode can be used for sterilization purposes to remove traces of bacteria, virus contaminants and protein aggregates [8].

A.

B.
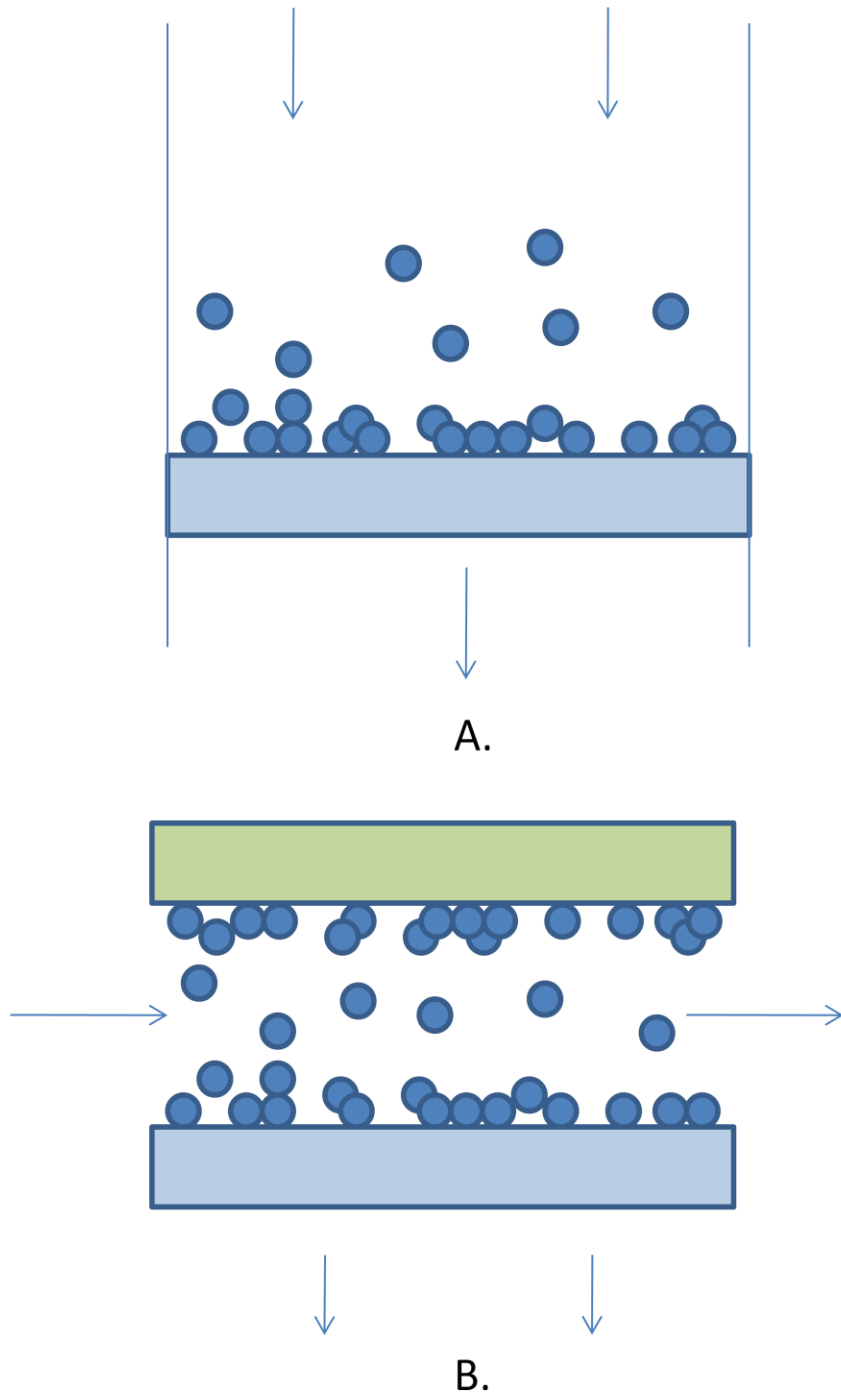
Figure 1: Two types of setups for filtration: A) Dead end filtration, and B) Tangential flow filtration

2.3 PROTEIN FOULING: ADSORPTION & DEPOSITION

There are many applications where microfiltration is used and many of these include protein solutions. Unfortunately it has been shown that when proteins are present there is a significant amount of fouling. This leads to a decrease in membrane performance and possible loss of product. Because of this, many membranes need to be replaced due to fouling. Since this is so critical in filtration processes, there has been a substantial amount of research done on membrane fouling due to proteins [9].

When talking about adsorption and deposition, normally these refer to the proteins being adsorbed or accumulating onto the edges of membrane pores and the membrane surface [9, 10]. By focusing on the accumulation of particulates, protein fouling can be classified based on two locations. There is external fouling that occurs when there is accumulation on the surface of the membrane and then there is internal fouling which is the increase in particulates within the pores [9- 11]. However, since microfiltration membranes have pores that are much greater than the diameter or the proteins, it was thought that the adsorption of particulates to the edges of membrane pores is not as significant in the fouling process. It was also believed that during microfiltration, the internal and external methods of fouling occur simultaneously [10].

Adsorption of proteins can be studied based on "static adsorption" methods. This occurs when no pressure is applied and is governed solely on diffusion. In this case, it was determined that the amount of protein adsorbed onto the membrane was linearly related to the adhesion force [10]. It was observed that a monolayer of protein was adsorbed to the surface. Many dynamic methods were tested as well, because the adsorption method was expected to be different than the static adsorption. When a protein solution was pumped through a membrane, they observed cake layers of protein and determined that the fouling appeared to be occurring at the surface [10]. This was for all membranes, even when they collected a significant amount of protein in the permeate.

2.4 FACTORS THAT CAUSE PROTEIN FOULING DURING MICROFILTRATION

During microfiltration, there are many conditions that can play significant roles in protein fouling. The pH of the solution being filtered, the feed pressure, concentration of the feed solution, amount of aggregates in the solution, surface chemistry of the membrane, and the membrane morphology all have an effect on protein fouling during microfiltration.

(i) pH

The pH of the bulk solution has an effect on the amount of protein fouling the membranes. The pH of the solution can be above, below, or at the isoelectric point. The isoelectric point is where there is no net charge [4]. When the pH is below the isoelectric point, the proteins are positively charged and if the pH is above the isoelectric point the proteins are negatively charged [12].

Zhang *et al* [10] found that the maximum adsorption of protein onto the membrane occurred at the isoelectric point. When the solution is at the protein's isoelectric point this is the least amount of repulsion between molecules. At this pH, they found that protein molecules were easily adsorbed onto the membrane as well.

Similarly, Palecek and Zydney [13] found that at the protein isoelectric point the permeability is at a minimum. The permeability decreases when the salt concentration increases at pH's above and below the isoelectric point.

Velasco *et al* [14] also observed that when there is no charge attraction between the protein and membrane, the membrane is less likely to foul. They say they need a high pressure to have any fouling occur. When the bulk solution is at the protein's isoelectric pH, they expected to see a high amount of aggregates form and foul the membrane.

Palecek and Zydney [15] found that the flux increased as the pH moved farther away from the protein's isoelectric pH. This helps to prove that at the isoelectric point, the flux decline is the most severe. When the pH was below the isoelectric point of the protein, the flux and protein transmission were high.

It was found that at the isoelectric point, the protein aggregation and adsorption were at their greatest. However, they do point out that it is possible to have high levels of denaturation and aggregation at pH values below the isoelectric point when the solution is most acidic.

(ii) Feed Pressure

The feed pressure is the driving force in an experiment. In filtration, the pressure forces the fluid through the membrane. A specific pressure may be essential to overcome membrane resistance and provide a certain flux through the membrane [16]. Many studies have used a variety of pressures to better determine what conditions lead to greater fouling and a decrease in flux. Palecek and Zydney [13] found that when using BSA, the hydraulic permeability decreased as the applied pressure increased.

Velasco et al [14] studied how different applied pressures affect the fouling mechanism of BSA. They found that at low applied pressures, the fouling was more internal while at high pressures, a cake layer begins to form externally on top of the membrane surface.

Tunga *et al* [16] state that the permeate flux increases as the pressure increases. The flux can be affected when fouling by cake filtration occurs. When higher pressures are used, it is possible that this cake layer can become compressed which increases resistance and leads to a decrease in flux.

(iii) Concentration

Tracey and Davis's [17] results helped to show that at low concentrations of BSA, internal fouling occurred while at a much higher BSA concentrations, external fouling took place. They determined that when a protein solution is at a high concentration, there are more aggregates present and they are much larger aggregates. Because of this, they tend to form a coating on the surface of the membrane.

Güell and Davis [18] ran experiments at different concentrations of BSA, ovalbumin, and lysozyme. In particular they found that ovalbumin had the greatest amount of flux decline and this flux decrease was even greater with higher protein concentration. They believe that this helps

to prove that there are larger and more numerous aggregates in solutions that have a higher concentration of protein.

Mueller and Davis [19] found that when they increased the concentration of the protein in solution, this led to a faster transition to external membrane fouling. At low concentrations, fouling would begin with internal fouling and later switch to external fouling.

(iv) Aggregation

Aggregation of proteins that accumulate on the membrane surface have been considered a major factor in fouling [9]. Many studies have researched the presence of aggregates found in protein solution. Chandavarkar and Coony had discovered that the flux decline in their system was due to deposition of large BSA aggregates from the bulk solution. They were able to come to this conclusion using quasi-elastic light scattering. The aggregates were formed because of prolonged pumping that was needed to drive the solution through the membrane [9, 18].

Another helpful discovery related to aggregates in bulk solution was published by Güell and Davis [18]. They found that at higher protein concentrations there are more aggregates formed compared to lower protein concentrations.

Kelly *et al* [20] discovered that the fouling of microfiltration membranes by BSA was related to the deposition of aggregated and/or denatured protein. They determined that these aggregates provide a site for nucleation where other particulates begin to deposit. From these findings they hypothesized that there were two steps that effected flux decline. The first step was that these BSA aggregates were deposited on the membrane surface which first affects the flux. Next the protein in the bulk solution would attach to these aggregates and further lead to fouling and a decrease in flux.

To help reduce the amount of aggregates in bulk solution many experiments used some sort of pre-filtration. Kelly *et al* [20] used pre-filtration of a BSA solution before microfiltration and more aggregates were removed by pre-filtering the solution in smaller and smaller molecular weight cut-off membranes.

Kanani *et al* [8] compared experiments that were run with pre-filtered solutions and non pre-filtered solutions. Cellulose acetate membranes with a nominal pore size of 0.45 μm were used for the filtration experiments. They found that after pre-filtering the feed solution, there was minor fouling apparent on the membrane surface. They had initially hypothesized that aggregates in the protein solution were responsible for the membrane fouling and when they pre-filtered the solution, these aggregates were removed. They found that the fouling was caused by the protein monomer that would attach to the aggregates on the surface of the membrane.

(v) Surface Chemistry

Membranes have been manufactured to have either a hydrophobic or hydrophilic surface chemistry. When a membrane is hydrophobic, water tends to bead up on the surface. If the membrane is hydrophilic then a droplet of water will spread out over the surface. Water contact angle measurements are used to help determine if a membrane is a hydrophobic or hydrophilic membrane. In these measurements a water droplet is dropped onto the surface of the membrane and the angle at which the droplet meets the membrane determines if it is hydrophilic or hydrophobic. When the angle is larger than 90° the membrane is hydrophobic and when the angle is close to 0° then the membrane is hydrophilic.

Many people are studying the effects of different surface chemistries on membranes. From this research it has been determined that if a membrane is hydrophobic it is more likely to have protein adsorption than a hydrophilic membrane [18]. This is such a widely researched area because it would be useful to have a property that is able to better control the rate of fouling.

Maximous *et al* [21] compared the flux decline of two different types of membranes, a hydrophobic membrane (PES) and a hydrophilic membrane (regenerated cellulose). They showed that the hydrophobic membrane had greater protein rejection and lower flux than the hydrophilic membrane. The hydrophobic membrane was found to have a cake layer built up on the surface.

Jönsson and Jönsson [22] also studied the effects of hydrophobic versus hydrophilic coating on membrane surfaces. They found that the flux had a significant decline when using

hydrophobic membranes, but when using hydrophilic membranes the flux only had a minor reduction in flux. Also they found that the type of surface chemistry on the membrane has an impact on the flux when running solutions that contain hydrophobic solutes.

Boussu *et al* [23] found that when a membrane has a hydrophilic smooth surface then this is beneficial in reducing the amount of fouling that occurs on the membrane.

(vi) Membrane Morphology

The structure of the membrane plays an important role in the method of separation and a way to classify the type of membrane. For ceramic and polymeric membranes, the pores in a microfiltration membrane are able to filter particles ranging from 0.1-10 μm so that smaller particles are able to pass through [4, 16]. The synthetic membranes can be organized into two groups called either symmetric or asymmetric membranes.

Symmetric membranes received this name because throughout the thickness of the membrane, it is uniformly isotropic. Symmetric membranes can then be broken down based on if the membrane consists of cylindrical pores, a porous texture, or a nonporous uniformity. Usually the second two can have a membrane thickness that ranges from 10 to 200 μm [4]. The pore size distribution and thickness of the membrane help to determine how permeable the membrane is and retention is based on the surface of the membrane [7].

Asymmetric membranes are also porous but they are anisotropic. These membranes have a dense layer on the top of the membrane which is only 0.1 to 0.5 μm thick [4]. This top layer is supported by the lower section which can be 50- 150 μm thick. This bottom layer is considered the porous membrane. These membrane can have a change in porosity, pore size or membrane composition throughout the membrane [5]. PVDF is an example of an asymmetric membrane that is produced by the phase inversion method [24].

Ho and Zydney published two articles [25, 26] that used track-etched, isotropic and asymmetric microfiltration membranes to determine how the membrane morphology and pore structure had an effect on the amount of fouling. In this study they found that with membranes

with straight through pores such as track-etched membranes, had fouling occurring by deposition of protein aggregates. The amount of pore blockage that occurred was also related to the membrane porosity because if a membrane had high porosity, the aggregates were more likely to block multiple pores. They also found that the membranes that had interconnected pores had a lower fouling rate since the fluid had alternate ways to flow around blocked pores. The last type of membrane they studied was the asymmetric membrane. Their results showed that asymmetric membranes performed as though it had straight-through pores that were not connected. Overall, they were able to show that interconnected pores had a significant effect on flux decline.

Güell and Davis [18] found that microfiltration membranes that had a low porosity had higher fouling since the pores could be easily blocked by foulants. As expected, when they used membranes with a more open morphology, such as cellulose acetate and PVDF, there were lower fouling rates since the pores were not as easily blocked by aggregates.

2.5 FOULING MECHANISM MODELS

There are four blocking models that are based on Darcy's Law; complete blocking, standard blocking, intermediate blocking, and cake filtration. Some researchers tend to group complete and intermediate blocking so there are three groups; pore blockage, pore constriction or cake filtration. The four models are shown in Figure 2.

In 1935, Hermans and Bredée were the first researchers to publish information on blocking filtration mechanisms [27, 28]. Since then, many people have studied and continue to study the complexity of the mechanism of blocking. While these blocking laws have been around for quite awhile, the last one to be discovered was the intermediate blocking law. Hermia [27] has the first article that includes the intermediate blocking law and in this paper each of the four blocking mechanisms are derived. Each blocking model was found to simplify down to the Equation 1 shown below. Each model has different equations that are equal to α, and then different values for β which are constants. These β values are shown in Table 1 below. By

plotting the log of d^2t/dV^2 versus the log of dt/dV, this results in producing a linear graph with the

slope of β. Since each of the blocking models have different β values, the slope from the graph

can be matched with the blocking model to determine the mechanism of fouling. The assumptions

related to each of these models in shown in Table 2.

$$\frac{d^2t}{dV^2} = \alpha \left(\frac{dt}{dV}\right)^{\beta}$$

Equation 1: Simplfied form of Darcy's Law to help predict fouling mechanism models.

Blocking method	β
Complete	2
Standard	3/2
Intermediate	1
Cake	0

Table 1: The β values corresponding to the type of blocking method.

Complete Blocking	Pore is entirely blocked by solute
Standard blocking	Solute deposits evenly along pore walls
Intermediate blocking	Pores are partially blocked by solutes with a certain probability
Cake filtration	Cake layer of solutes develop on the surface of membrane

Table 2: The assumptions given about each of the types of blocking methods.

These blocking laws continued to be studied and over time researchers began to modify

the mechanisms based on new findings. Ho and Zydney [29] found that a combination of the pore

blockage models and cake filtration models was more adequate. When referring to pore blockage,

this includes complete and intermediate blocking. They developed a different mathematical

model that relates the fouling that occurs initially which is due to pore blockage and the fouling

due to cake layer buildup after the initial blockage. This model was able to relate the run time to the thickness of the cake layer over the membrane. They also performed experiments with BSA filtered through 0.2 μm pores of polycarbonate track-etched membranes, which have straight through pores, to determine how well the model corresponds to experimental data. They found that the model precisely fit the experimental data. This mathematical model was able to give a transition between the pore blockage to cake layer buildup during protein filtration.

Not long after this, another article by Ho and Zydney which also included Palacio [30] was published which looked closer at this new combined model with several different proteins. Five different proteins were chosen and a polycarbonate track-etched membrane with 0.2 μm pores was used to filter each of the protein solutions. In this case they did not use any pre-filtration membranes as they did in their previous experiment with BSA [29]. They found in this study that the initial flux decline was caused by large aggregates leading to pore blockage. They then found that there was a transition to cake filtration and that the combined model discovered earlier was in good agreement of the data obtained experimentally.

An article was published by Bolton *et al* [31] that took the idea of the combined blocking models and expanded upon this by combining each individual blocking method. Five models were discussed; cake filtration-complete blocking, cake filtration-intermediate blocking, cake filtration-standard blocking, complete blocking-standard blocking, and intermediate blocking-standard blocking. They found that the cake-filtration-complete blocking model had the best fit to experimental data, but they thought the other models would also useful.

Duclos-Orsello *et al* [1] purposed a three mechanism model. They use the terminology of pore blockage, pore constriction, and cake filtration. Complete and intermediate blocking are combined in the term pore blockage and standard blocking is renamed as pore constriction. They combine all three of these mechanisms into a model. This was similar to the original combined model discovered by Ho and Zydney [29], but this included pore constriction in the model. They say that first, pore constriction will take place and then this will transition to pore blockage which

will dominate. This will then result in cake filtration over time. They first used 0.25 μm polystyrene microspheres to mimic a protein. They filtered the polystyrene through 0.22 μm Isopore membranes. Next they experimented with BSA filtered through hydrophobic Durapore membrane. The model was used to help determine the proportion that each mechanism effected the overall filtration. This new model was able to provide the importance of each mechanism in the fouling process.
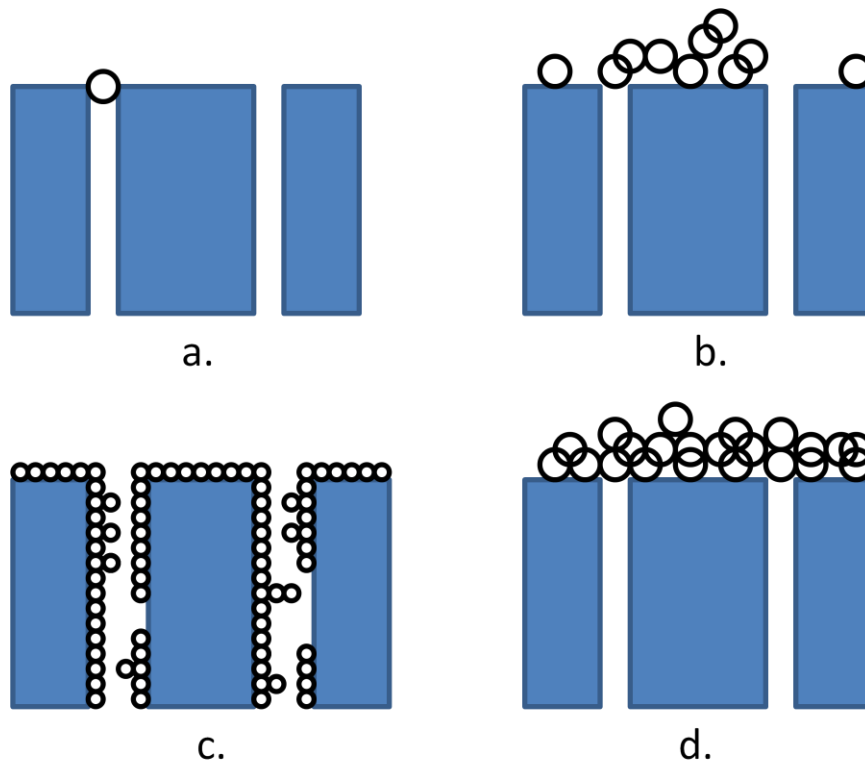
Figure 2: Four mechanisms of fouling: a) Complete blocking, b) Intermediate blocking, c) Standard blocking, d) Cake filtration.

CHAPTER 3. MATERIALS AND METHODS

3.1 MATERIALS

(i) Membranes

The two different microfiltration membranes used in experiments were poly (tetrafluoroethylene) (PTFE) provided by W.L. Gore & Associates, Inc., Newark, DE and poly (vinylidene fluoride) (PVDF) obtained from Millipore, Bedford, MA. Both PVDF and PTFE have a nominal pore size of 0.45 µm. These membranes were uncoated PTFE and uncoated PVDF. Since these are both hydrophobic in their uncoated state, W.L. Gore & Associates used polyvinyl alcohol (PVA) to coat both PTFE and PVDF to change the surface chemistry of the membrane to hydrophilic. The uncoated PTFE and PVDF and PVA coated PTFE and PVDF were each used for this project.

Three other membranes were used as pre-filters for the protein solutions. A nylon membrane called Nylaflo^{TM} with a nominal pore size of 0.2 µm was supplied by Pall, Ann Arbor, MI. The uncoated PTFE membrane with a nominal pore size of 0.45 µm was supplied by W.L. Gore & Associates, Newark, DE. The third pre-filter was Whatman Grade No. 1 Filter Paper with approximately 1µm nominal pore size.

(ii) Proteins

The three following powdered proteins were used in experiments and were obtained from Sigma-Aldrich, St. Louis, MO: (i) lysozyme (L6876, lysozyme from chicken egg white, lyophilized), (ii) β-lactoglobulin (L2506, β-lactoglobulin from bovine milk, lyophilized powder), and (iii) ovalbumin (A5378, albumin from chicken egg white, lyophilized powder). Additional

experiments were done using hemoglobin (H2500, bovine blood hemoglobin, lyophilized powder). Each of these proteins is globular.

Lysozyme is an important enzyme and is used for many different applications such as a food additive for milk products, a cell-disrupting agent, a drug for treatment of ulcers and infections, a component in ophthalmologic preparations, and may have a potential use as an anticancer drug [32]. Although lysozyme is found in many sources, it occurs naturally in chicken egg white [32]. It is a small globular protein and it is highly cationic [33]. The secondary structure of lysozyme is well characterized with 10% of it in the form of β-sheets and 39% in a helical structure which forms two domains [136].

Ovalbumin is a part of the serpin family which contains proteins that are known to inhibit proteases, however, ovalbumin lacks the ability to inhibit proteases [34, 156] . It is a glycoprotein that has 386 residues and it comprised 60-65% of total protein in egg white [156]. The tertiary structure has been studied and it has many β-sheets and α-helices structures [34]. However, the overall function of ovalbumin is not known. In commercial preparations of ovalbumin, the percent of native ovalbumin could range from 20-80% [34].

β-lactoglobulin is a small protein that exists as a dimer and is acid stable [36]. This protein is a major component in whey protein of milk and it is largely responsible for the aggregation of the whey protein [36, 48]. The secondary antiparallel β-strands make a lattice structure to form a tertiary structure [36, 48].

Hemoglobin has been well characterized since it is the protein that carries oxygen in red blood cells [47]. It has two identical alpha subunits and two identical beta subunits that are symmetrically arranged to form a quaternary structure [47].

Protein	Isoelectric Point	Molecular Weight
Ovalbumin	4.7	45 kDa
β-lactoglobulin	5.8	18.4 kDa
Lysozyme	11.0	14 kDa
Hemoglobin	7.2	68 kDa

Table 3: Properties of the four proteins

3.2 EXPERIMENTAL METHODS

(i) Preparation and Apparatus Set-up

Membrane fouling was studied using four proteins; lysozyme, β-lactoglobulin, ovalbumin and Hb. Each protein sample was weighed to give the desired protein concentration (0.1 or 2 g/L). The samples of lysozyme, β-lactoglobulin, and ovalbumin were prepared with 10 mmol phosphate buffer (monobasic (KH_2PO_4) & tribasic (Na_3PO_4): Fisher Scientific, Pittsburgh, PA, dibasic (Na_2HPO_4): Mallinckrodt Chemicals, Phillipsburg, NJ) at each of the proteins' corresponding isoelectric points by monitoring the pH change with a pH meter (Orion Model 420A). Monobasic is Hb was prepared using 0.15 M Phosphate Buffer Saline (PBS) (Fisher Scientific, Pittsburgh, PA). PBS consists for sodium chloride (81%), sodium phosphate dibasic (>14%), potassium phosphate monobasic (>3%), and potassium chloride (>2%). The Hb solution was then adjusted to the isoelectric point by adding 0.1 M NaCl or HCl. Each of the protein solutions were pre-filtered using 0.2 μm (Pall (Ann Arbor, MI)), 0.45 μm (PTFE base membrane, W.L. Gore, Newark, DE) and 1 μm (Whatman No. 1 Filter Paper) membranes to reduce aggregate formations.

Each filtration experiment was conducted in a 76 mm diameter Amicon stirred cell (Model 8400, Millipore, Bedford, MA). Although the container is called a stirred cell, the solution was not stirred. The membrane is fit into the bottom of the stirred cell and the feed solution is poured into the container, covering the membrane. Nitrogen gas was used to pressurize

the feed stream in the stirred cell. Depending on the desired pressure, 2 psi or 10 psi, the pressure regulator was adjusted accordingly. This pressure was maintained constant throughout the experiment. Based on the pressure, different effective membrane areas were used. When the pressure was at 2 psi, the effective membrane area was 41.8 cm^2. When the pressure was increased to 10 psi, a rubber gasket was placed over the membrane to reduce the effective membrane area to 20.9 cm^2. This reduction in area was useful to increase the run time of the experiment. All the experiments were run at 22-25°C.

Pre-filtration was conducted prior to beginning the experiment on each of the protein solutions that produced a significant flux decline when no pre-filtration step was performed. The experiments were done with the 0.2, 0.45, and 1 μm pre-filtration membranes. Each of these membranes was soaked in absolute ethanol to initially wet the membrane. The membranes were then placed in a stirred cell and flushed with 300 mL of deionized distilled water (Elga Prelab Ultra, 18.2 mΩ, 26.4°C). Then the stirred cell was filled with a protein solution. This solution was filtered and then set aside for use in the main filtration experiment. The concentration was determined before and after pre-filtration using a UV spectrophotometer (Thermo Scientific Genesys 10UV Scanning, Waltham, MA). Next the PTFE or PVDF membranes were also soaked in absolute ethanol to ensure wetting of the membrane. The membrane was placed in the stirred cell and flushed with 300 mL of deionized distilled water. Next a series of solutions were run through the PTFE or PVDF membranes. First the phosphate buffer specific to the protein was loaded into the stirred cell. Once all the phosphate buffer solution was forced through the membrane, the protein solution was loaded. All of the liquid from the protein solution was collected at regular intervals from the permeate to determine protein concentration and flux. Next the same phosphate buffer from the first step was used to flush the membrane. Fluxes for each of these steps was determined by recording the permeate weight from an electronic balance at regular intervals at the set pressure.
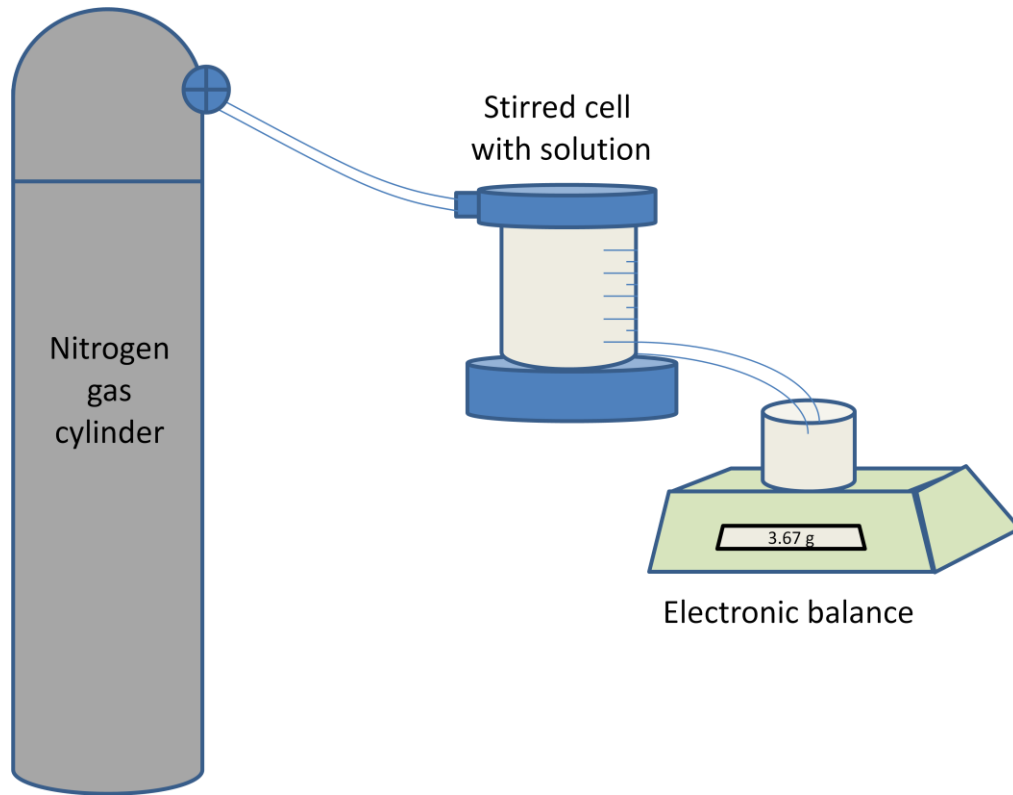
Figure 3: Representation of experimental setup with dead end flow filtration

(ii)Parameters

There were four main parameters investigated in this project: type of protein, feed pressure, protein concentration and nominal pore size of the pre-filtration membrane. There were four different types of proteins used, each at their respective isoelectic points: lysozyme, β-lactoglobulin, and ovalbumin. Additional experiments were done with hemoglobin at its corresponding isoelectric point. Two different feed pressures and two different protein concentrations were also investigated, 2 psi and 10 psi, and 0.1 g/L and 2g/L respectively. The protein solutions were pre-filtered using one of the three, 0.2 μm, 0.45 μm or 1 μm, nominal pore size membranes.

	Uncoated PTFE	PVA coated PTFE	Uncoated PVDF	PVA coated PVDF
ovalbumin	0.1 & 2 g/L, 2 & 10 psi	2 g/L, 2 & 10 psi	2 g/L, 2 & 10 psi	2 g/L, 2 & 10 psi
	no pre-filtration + 0.2, 0.45, & 1 μm pre-filtration	no pre-filtration + 0.2, 0.45, & 1 μm pre-filtration	no pre-filtration	no pre-filtration
lysozyme	0.1 & 2 g/L, 2 & 10 psi	2g/L, 2 & 10psi	2 g/L, 2 & 10 psi	2 g/L, 2 & 10 psi
	no pre-filtration	no pre-filtration	no pre-filtration	no pre-filtration
β-lactoglobulin	0.1 & 2 g/L, 2 & 10 psi	2 g/L, 2 & 10 psi	2 g/L, 2 & 10 psi	2 g/L, 2 & 10 psi
	no pre-filtration	no pre-filtration + 0.2, 0.45, & 1 μm pre-filtration	no pre-filtration	no pre-filtration

Table 4: Operating conditions and parameters for experiments.

(iii) UV Spectrophotometer

Each of the vials that contained the permeate protein solution were then used to determine protein transmission. Protein concentration in the permeate was measured at 280 nm absorbance using a UV spectrophotometer. Since only a small volume of permeate (2 mL) was needed from each sample, this gave only an estimate of the actual concentration in each sample. Permeate concentration versus collected permeate volume graphs were plotted and shown in Chapter 4. All analysis was done 22-25°C.

3.3 MEMBRANE SURFACE CHARACTERIZATION

(i) Attenuated Total Reflection-Fourier Transform Infrared Spectroscopy (ATR-FTIR)

ATR-FTIR has been used in many studies to help characterize the membrane surface. This method is able to detect absorptions in the infrared region 4000-400 cm^{-1} and the depth of penetration is on the order of a few micrometers (1-5 μm) [3, 4]. FTIR is a valuable to help determine the functional chemistry of an unknown substance. In this case it helps show if there something on the surface of the membrane such as protein deposits. The sample is placed against an internal reflection element [3]. The membrane samples are exposed to infrared light and during this time they absorb energy [37]. During each internal reflection, the infrared is able to penetrate into the sample which forms an evanescence wave [3]. The energy that is absorbed is related to

the vibrational energy in the atomic bonds [37]. Depending on the functional group, they each absorb energy at different wavelengths [37]. This results in an absorption spectrum which provides a unique fingerprint of the sample. A few well characterized spectral bands are 1600-1660 cm^{-1} which is called the amide I band and also a band around 1560 cm^{-1} which is known as the amide II band [37-39]. ATR is highly dependent on the contact between the membrane and the crystal surface. Since membranes are porous and have different roughnesses, this can have an effect on the optical efficiency [24]. The different sides of the membrane have been shown to produce considerably different spectra due to the morphology of the membrane [24]. ATR-FTIR spectroscopy (Nicolet FT-Raman Spectrophotometer, Waltham, MA) was used to analyze the surfaces of the clean and fouled membranes of the uncoated and PVA coated PTFE and PVDF membranes. The ATR-FTIR spectra were collected and analyzed with the Nicolet spectrometer. This contains a ZnSe crystal at a nominal angle of 45°. This gives about 12 internal reflections at the sample surface. The membrane is pressed against the ZnSe crystal in a vacuum tight container. This crystal provides a transmission range of 4000 to 600 cm^{-1}. Each sample had spectra collected with 128 scans at 4 cm^{-1} resolution. The background spectra was used to ratio the sample spectra and alignment was completed. All analysis was done at 22-25°C.

(ii) Field Emission Scanning Electron Microscopy (FESEM)

The scanning electron microscope is useful to examine and characterize the structure of membranes [4]. The resolution limit is around 10 nm and the membrane can be viewed from the top, bottom or cross-section [4]. The depth of analysis is only 0.5 nm [3]. FESEM figures are useful to determine the pore size, pore size distribution and porosity and comparisons between the figures are valuable even though it is only qualitative. There is a beam of electrons directed toward the sample and these are called the primary electrons [4]. Secondary electrons are released by the atoms on the surface of the membrane and collected by a detector. The sample is normally coated in a conducting layer to prevent charging from occurring and this helps avoid any damage of the sample [4].

Images of the clean and fouled membranes of the uncoated and PVA coated PTFE and

PVDF membranes were taken using FESEM (JEOL JSM-6500 F, Peabody, MA). This particular

FESEM has an In-Lens Thermal Field Emission Electron Gun (TFEG). Each of the membranes

was dried in the oven for 3 hours at 45°C. Approximately 4 mm by 4 mm sections were taken

from the membrane and attached to a pin stub with magnetic tape. These stubs were then placed

in a desiccator overnight to ensure that the membranes would stay dry. Next the membranes were

gold sputter coated (Hummer VII, Anatech LTD, Alexandria, VA) with 10 nm thickness. Each of

the stubs containing the gold sputter coated membranes was then secured in a holder which was

placed in the chamber to view with FESEM. Each of the images was taken at 2500x

magnification. These images of the clean and fouled membranes were then compared to

determine extent of fouling.

CHAPTER 4. RESULTS AND DISCUSSION

4.1 PHOSPHATE BUFFER FLUX

      Each of the membranes, uncoated and PVA coated PTFE and PVDF were tested at two different pressures; 2 psi and 10 psi. To determine the permeate flux of each membrane, the phosphate buffer specific to each protein depending on isoelectric point was run through each membrane. It was found that the pH of the buffer does not have a significant effect on the flux so only one set of data is shown for the high and low pressure of each membrane. The permeate flux of the buffer as a function of permeate volume for uncoated and PVA coated PTFE is shown in Figure 4 and the uncoated and PVA coated PVDF fluxes are shown in Figure 5. The phosphate buffer fluxes are relatively constant during filtration. For the uncoated PTFE membrane, when the feed pressure is at 2 psi, the permeate flux is around 2,000 L/m^2hr but when the feed pressure is at 10 psi the permeate flux is around 8,000-9,000 L/m^2hr. The PVA coated PTFE membrane has a slightly lower permeate flux for both 2 psi and 10 psi. At 2 psi the permeate flux is around 1,000 L/m^2hr while at 10 psi the permeate flux is around 6,000-7,000 L/m^2hr.

      For the uncoated PVDF membrane, when the feed pressure is at 2psi, the permeate flux is around 1,400 L/m^2hr but when the feed pressure is at 10psi the permeate flux is around 7,000-8,000 L/m^2hr. The PVA coated PVDF membrane also has lower permeate flux for both 2psi and 10psi. At 2psi the permeate flux is around 1,200 L/m^2hr while at 10psi the permeate flux is around 6,000-7,000 L/m^2hr.These figures demonstrate that an increase in feed pressure also increases the phosphate buffer permeate flux. Since there is a fivefold difference in the pressures, there should be a fivefold difference in the flux values. When the flux at 2 psi is 2,000 L/m^2hr the flux at 10psi should be 10,000 L/m^2hr.

These values are slightly lower at 10 psi which could be due to compaction of the membrane at higher pressures. From these figures, the initial flux of the PVA coated membranes is lower than for the uncoated membranes. This same flux decrease has been shown to be the case with surface-modified polyethylene and polypropylene versus the unmodified membranes due to the hydrophilic coating contracting when the membrane is dry versus expanding when the membrane is wet [19]. By coating a membrane this changes the surface so that the pore sizes are reduced. PVA membranes have been found to highly swollen in water [46].
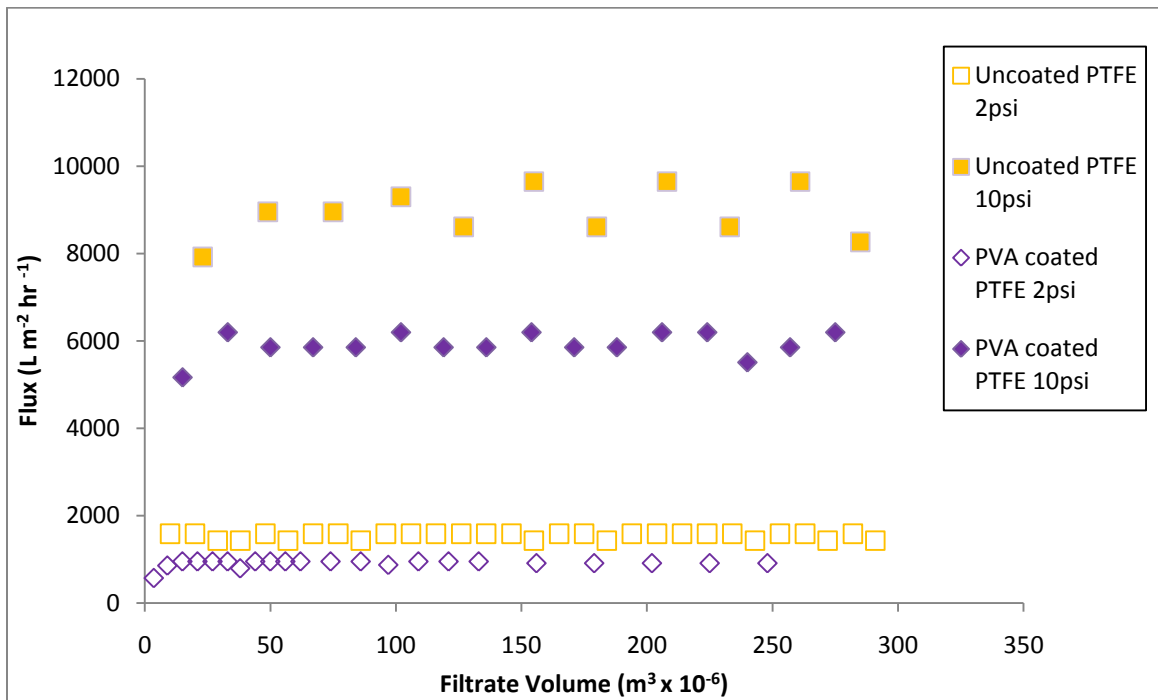

Figure 4: Buffer permeate flux versus filtrate volume determined by filtering through 0.45 μm uncoated and PVA coated PTFE membrane.
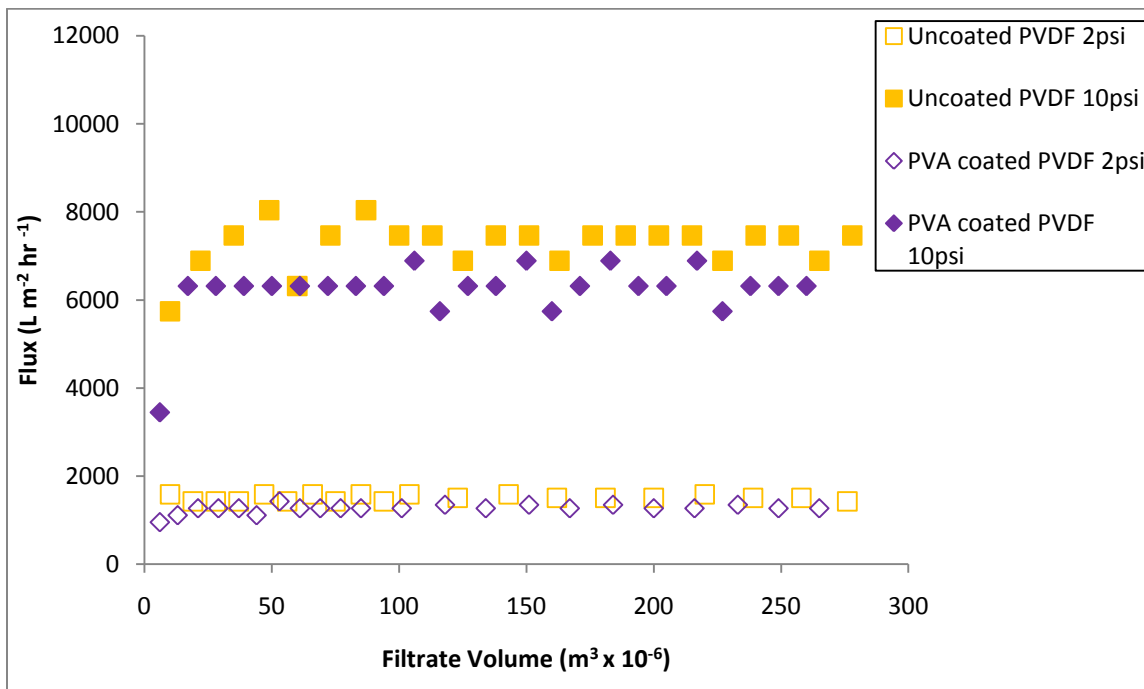
Figure 5: Buffer permeate flux versus filtrate volume determined by filtering through 0.45 μm uncoated and PVA coated PVDF membrane.

4.2 UNCOATED PTFE & HYDROPHILIC COATED PTFE MEMBRANES

4.2.1 Protein Flux

(i) Effect of Type of Protein

The effect of lysozyme, β-lactoglobulin and ovalbumin on the permeate flux decline for uncoated PTFE membranes are shown in Figure 6. Although the concentration 0.1 g/L was tested at 2 psi and 10 psi for each of the proteins, there was no flux decline seen and the graph appears similar to the phosphate buffer permeate flux versus permeate volume plots in Figure 4. The initial permeate flux for each of the proteins at the feed pressure of 10 psi is around 8,000 L/m^{2}hr. The initial permeate flux of each of the proteins for the lower feed pressure of 2 psi is about 1,500 L/m^{2}hr. These values agree with the values of the phosphate buffer flux for uncoated PTFE. From this figure the only protein that shows a significant decrease in flux is ovalbumin. Since the other two proteins have fairly constant flux values with increasing volume, pre-filtration is not necessary.

The three proteins lysozyme, β-lactoglobulin, and ovalbumin were all filtered through PVA coated PTFE at 2 g/L 2 psi and 2 g/L 10 psi. Each of the different conditions is shown in Figure 7. At 2 psi each of the proteins have a permeate flux that is initially about 1,000 L/m^2hr. When the protein solution has a feed pressure of 10 psi, the permeate flux is initially about 6,000 L/m^2hr. These values correspond with permeate flux values for the phosphate buffer. β-lactoglobulin and ovalbumin both show a significant decrease in flux as the permeate volume increases. Lysozyme, however, has fairly constant flux at both low and high pressure as permeate volume increases. At both 2 psi and 10 psi ovalbumin and β-lactoglobulin show a flux decline. Ovalbumin has a much more drastic change in flux, while β-lactoglobulin has a steady decrease in flux. This will be looked at more closely with the fouling mechanism models. While β-lactoglobulin has a flux decline at 2 psi, it is so gradual it is difficult to discern. By comparing lysozyme at 2 psi and β-lactoglobulin at 2 psi it is easier to detect the decline in flux for β-lactoglobulin.

Based on these results ovalbumin showed the greatest amount of fouling while lysozyme did not present any flux decline. A few articles which have studied these three proteins found comparable results. One study focused on BSA, lysozyme and ovalbumin. They determined that out of these three, ovalbumin had the greatest flux decline which they determined was from large aggregates in the ovalbumin solution [18]. Also this decrease in flux when filtering ovalbumin agrees with a study that used ceramic microfiltration membranes to filter ovalbumin [40]. In this study the rejection of ovalbumin at the isoelectric point was low because there were likely aggregates in solution that formed a gel layer on the surface of the membrane. Another study showed that lysozyme had the least amount of flux decline, while ovalbumin and β-lactoglobulin both had severe flux decline with 0.22 μm PVDF membranes [2]. Although these experiments were done with a different membrane, it still demonstrates the way each of the proteins foul in relation to the others. Ovalbumin and β-lactoglobulin have been found to aggregate by an intermolecular thiol-disulfide interchange reaction [2]. When there are already protein deposits on

the surface of the membrane, this reaction aids in chemically attaching the native protein to the aggregate [2]. This corresponds with the flux results showing ovalbumin and β-lactoglobulin having the greatest amount of flux decline.

Normally, it has been shown that a hydrophilic surface does not have as severe of a flux decline due to fouling [23, 41]. However, these results show that the hydrophilic PVA coated PTFE has a much more severe flux decline. One study did show that after modifying the surface of the membrane to be more hydrophilic, this actually decreased the pore sizes of the membrane and led to a lower flux [42].
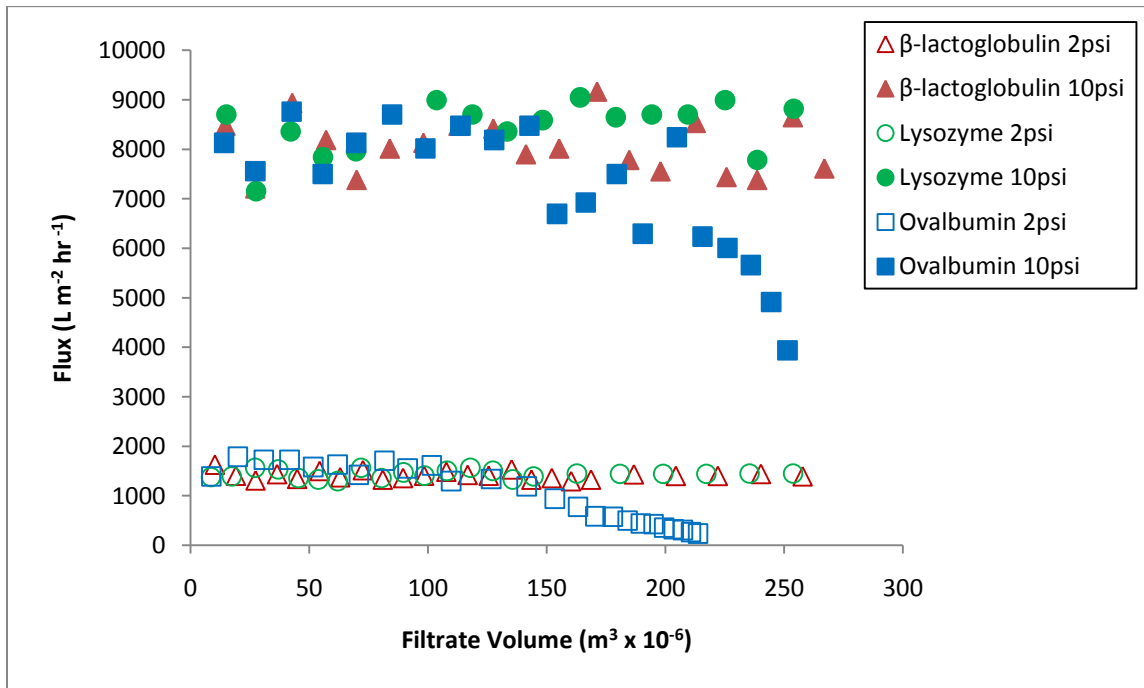

Figure 6: Permeate flux versus filtrate volume determined by filtering through 0.45 μm uncoated PTFE membrane. Protein solutions were prepared at isoelectric pH for the protein and operated at 2 psi and 10 psi. The permeate concentration of the protein was 2 g/L.
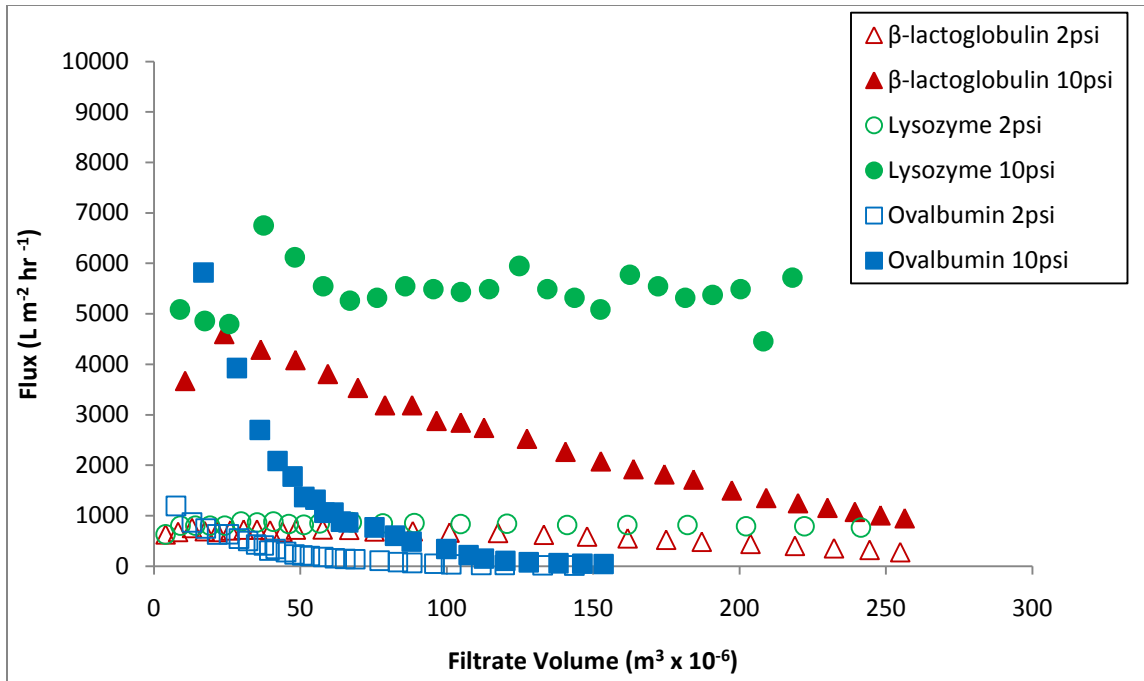
Figure 7: Permeate flux versus filtrate volume determined by filtering through 0.45 μm PVA coated PTFE membrane. Protein solutions were prepared at isoelectric pH for the protein and operated at 2 psi and 10 psi. The permeate concentration of the protein was 2 g/L.

(ii) Effect of Pre-filtration on Flux Decline

As discussed previously, aggregates are well known to initially deposit on the membrane and result in a flux decline. Once these aggregates are removed with pre-filtration, this has been proven effective in helping to eliminate protein fouling [2] and results shown in Figure 8, Figure 9, and Figure 10 help to support this claim. Also the concentration was taken before and after pre-filtration and the protein concentration decreased after pre-filtration. This means that some of the protein, which was likely the protein aggregates, was filtered out by the pre-filtration membranes. These values are shown in Appendix A.

The effects of the different pre-filtration nominal pore sizes on the permeate flux decline of ovalbumin for uncoated PTFE membranes are shown in Figure 8. Since only ovalbumin showed a decrease in flux in Figure 6, ovalbumin was focused on for pre-filtration. The 1μm nominal pore size pre-filtration membranes were shown to be comparable to no pre-filtration. With this large pore size, it may reduce the amount of aggregates slightly, but continues to show a

flux decline. There is still a significant flux decline when the ovalbumin solution was pre-filtered with 1 μm. However, with 0.45 μm or 0.2 μm nominal pore size pre-filters; there is no flux decline present.

The effects of the different pre-filtration nominal pore sizes on the permeate flux decline of ovalbumin and β-lactoglobulin for PVA coated PTFE membranes are shown in Figure 9 and Figure 10. Pre-filtration was conducted on ovalbumin and β-lactoglobulin, since these two showed a decrease in flux in Figure 7. The 1 μm nominal pore size pre-filtration membranes were shown to be comparable to no pre-filtration. With this large of pore size it may take out the largest aggregates but does not have any effect on the overall filtration. For both ovalbumin and β-lactoglobulin there is a significant flux decline when the solutions were pre-filtered with 1 μm. However, with 0.45 μm or 0.2 μm nominal pore size pre-filters, there does not appear to be a considerable flux decline. Ovalbumin may have a slight flux decline after pre-filtering with 0.2 μm or 0.45 μm, but it is difficult to determine. β-lactoglobulin may also have a very small flux decline with increasing volume with 0.45 μm pore size pre-filter.

Pre-filtration was also conducted on Hb solutions and filtered through uncoated and PVA coated PTFE. The flux results are shown in Appendix A. This graph also shows that when pre-filtering with 0.45 and 0.2 μm pore sizes, there is no flux decline observed.
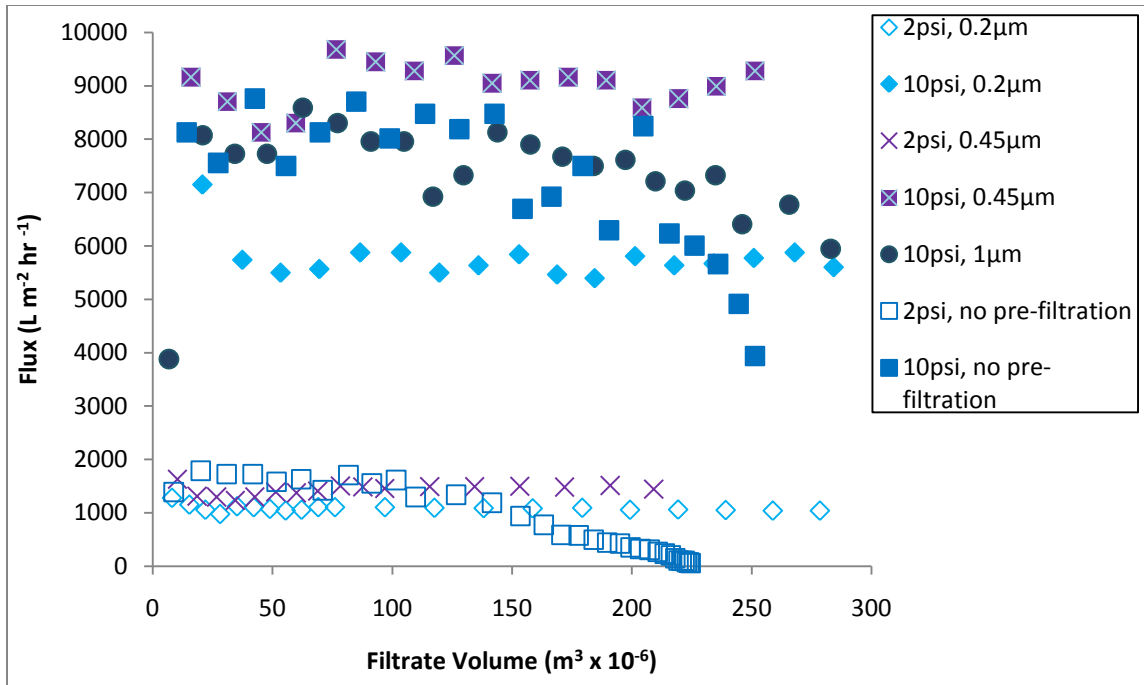
Figure 8: Ovalbumin permeate flux versus filtrate volume determined by filtering through 0.45 μm uncoated PTFE membrane. Ovalbumin solutions were prepared at pH 4.7 and operated at 2 psi and 10 psi. Ovalbumin permeate concentration was 2g/L.
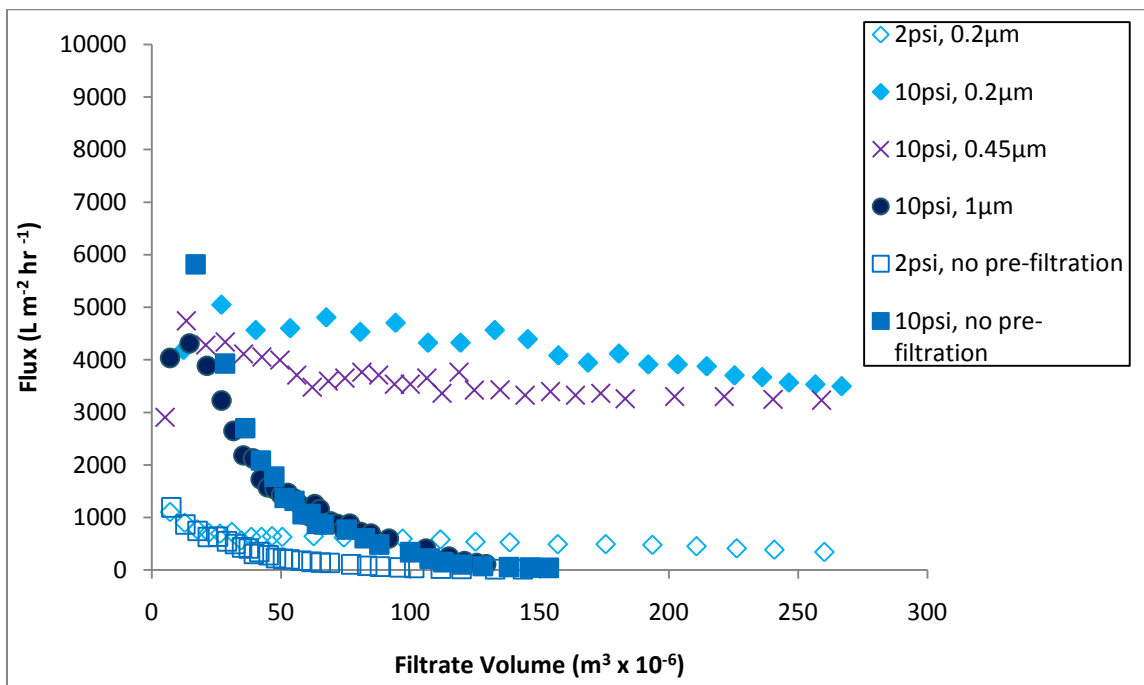

Figure 9: Ovalbumin permeate flux versus filtrate volume determined by filtering through 0.45 μm PVA coated PTFE membrane. Ovalbumin solutions were prepared at pH 4.7 and operated at 2 psi and 10 psi. Ovalbumin permeate concentration was 2 g/L.
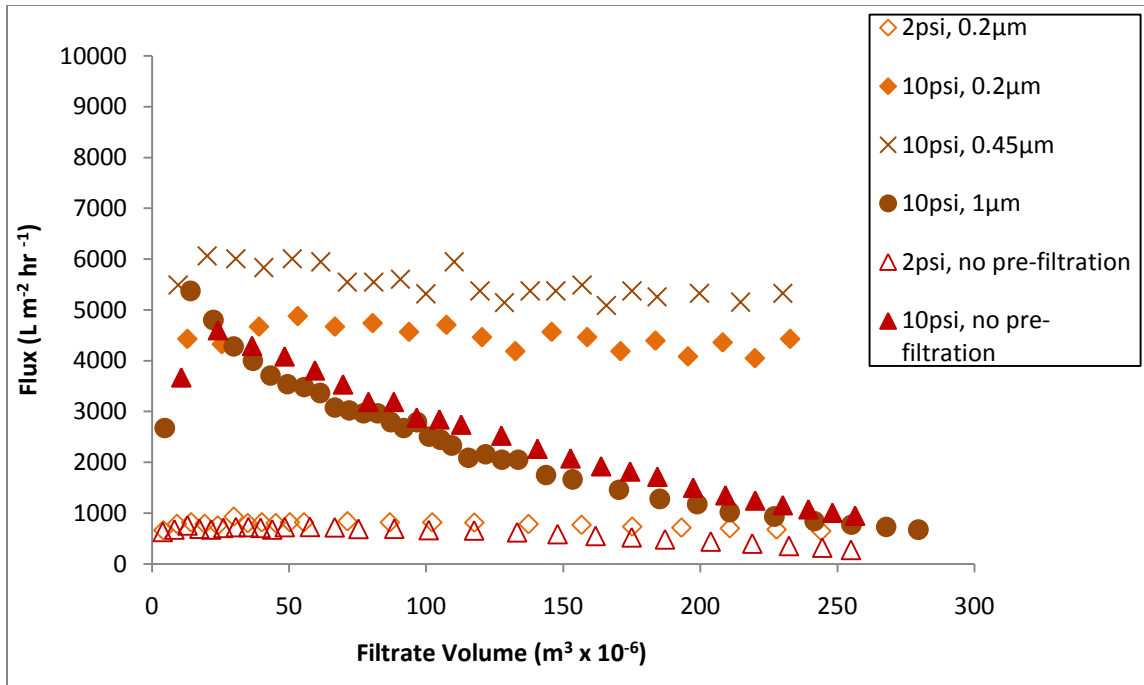
Figure 10: β-lactoglobulin permeate flux versus filtrate volume determined by filtering through 0.45 μm PVA coated PTFE membrane. β-lactoglobulin solutions were prepared at pH 5.8 and operated at 2 psi and 10 psi. β-lactoglobulin permeate concentration was 2 g/L.

(iii) Effect of Feed Pressure on Flux

The effect of feed pressure on permeate flux is shown in Figure 11, Figure 12 and Figure 13. The permeate flux of each protein and each membrane increases when the feed pressure is at 10psi rather than 2 psi. This is the same trend as was seen with the phosphate buffer flux. When the feed pressure is 10psi, the average permeate flux was 8,000 L/m^{2}hr for uncoated PTFE and around 6,000 L/m^{2}hr for PVA coated PTFE. When the feed pressure was 2psi, the average permeate flux was 1,500 L/m^{2}hr for uncoated PTFE and 1,000 L/m^{2}hr for PVA coated PTFE. These trends with the pressure were expected based on findings by Paleck and Zydney [13], Velasco *et al* [14], and Tunga *et al* [16].

(iv) Effect of Initial Protein Concentration on Flux (Only Uncoated PTFE)

Two different protein concentrations were studied to determine the effect the concentration has on permeate flux. For lysozme, β-lactoglobulin and ovalbumin the low concentration was 0.1 g/L and the high concentration was 2 g/L. Based on Figure 11, Figure 12

and Figure 13, when the low concentration was used, the permeate flux remained constant. The permeate flux was initially the same for both 0.1 g/L and 2 g/L at 2 psi. The same was seen at 10 psi.

Only ovalbumin in Figure 11 had any flux decline at 2 g/L and both pressures. As discussed previously, the higher the concentration of protein, there is a high concentration of aggregates present in the solution [18]. Since the high concentration, 2 g/L, produced a flux decline with increasing volume, the remaining experiments were focused on the high concentration.
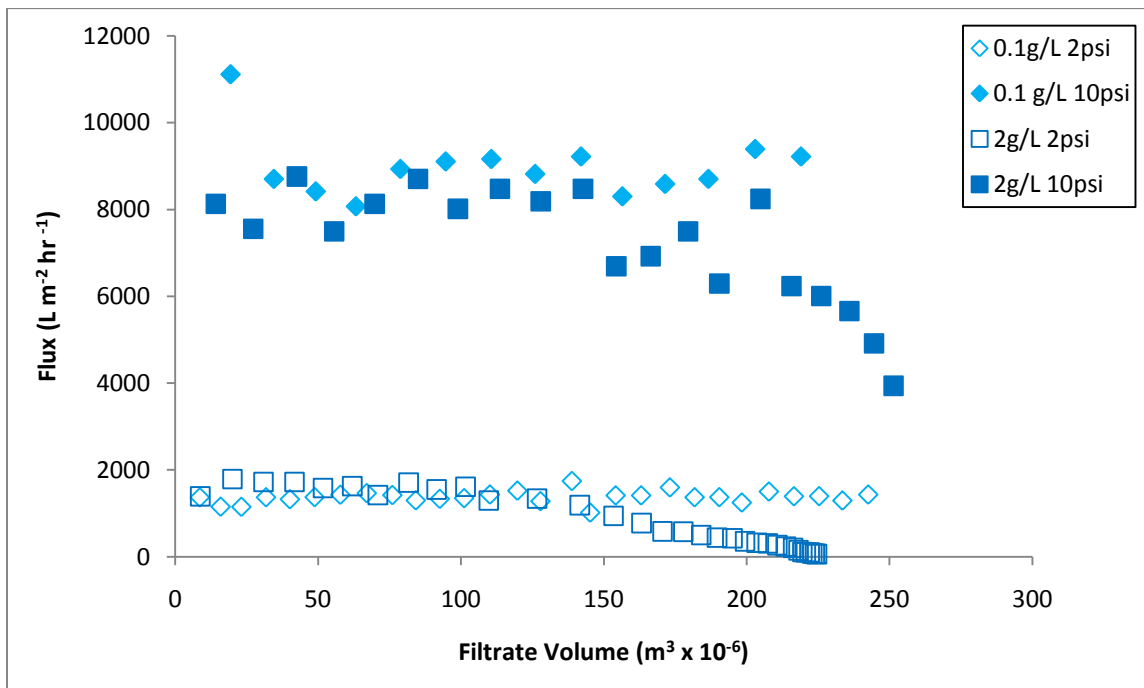

Figure 11: Ovalbumin permeate flux versus filtrate volume determined by filtering through 0.45 μm uncoated PTFE membrane. Ovalbumin solutions were prepared at pH 4.7 and operated at 2 psi and 10 psi. Ovalbumin permeate concentration was 0.1 g/L and 2 g/L.
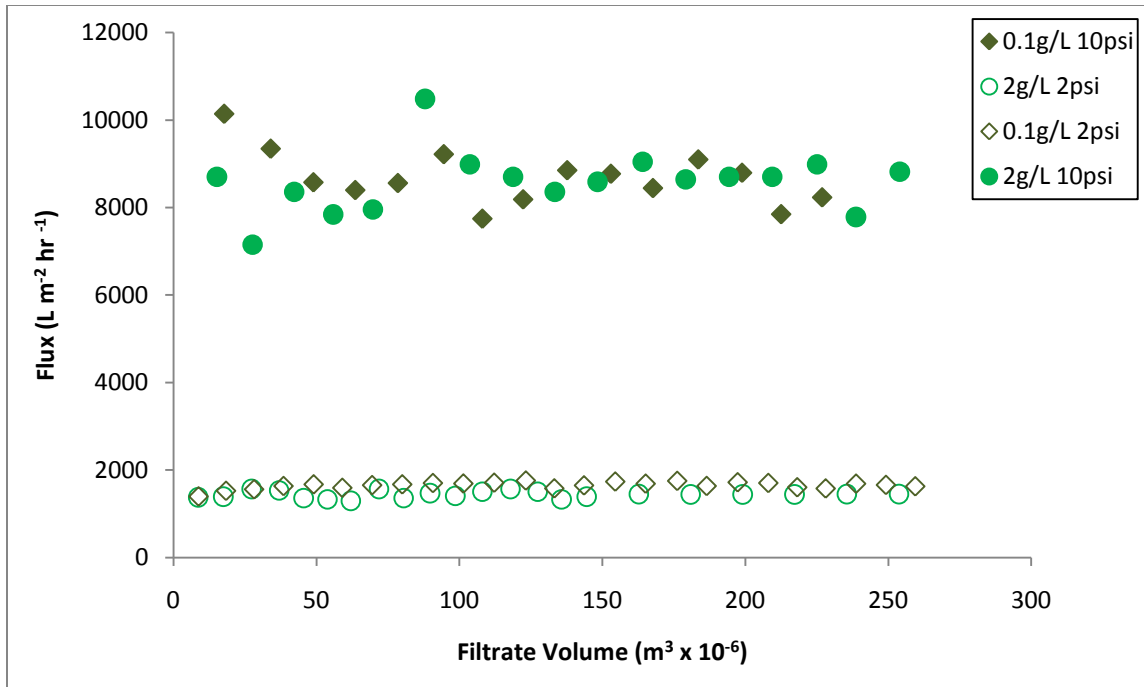
Figure 12: Lysozyme permeate flux versus filtrate volume determined by filtering through 0.45 μm uncoated PTFE membrane. Lysozyme solutions were prepared at pH 11.0 and operated at 2 psi and 10 psi. Lysozyme permeate concentration was 0.1 g/L and 2 g/L.
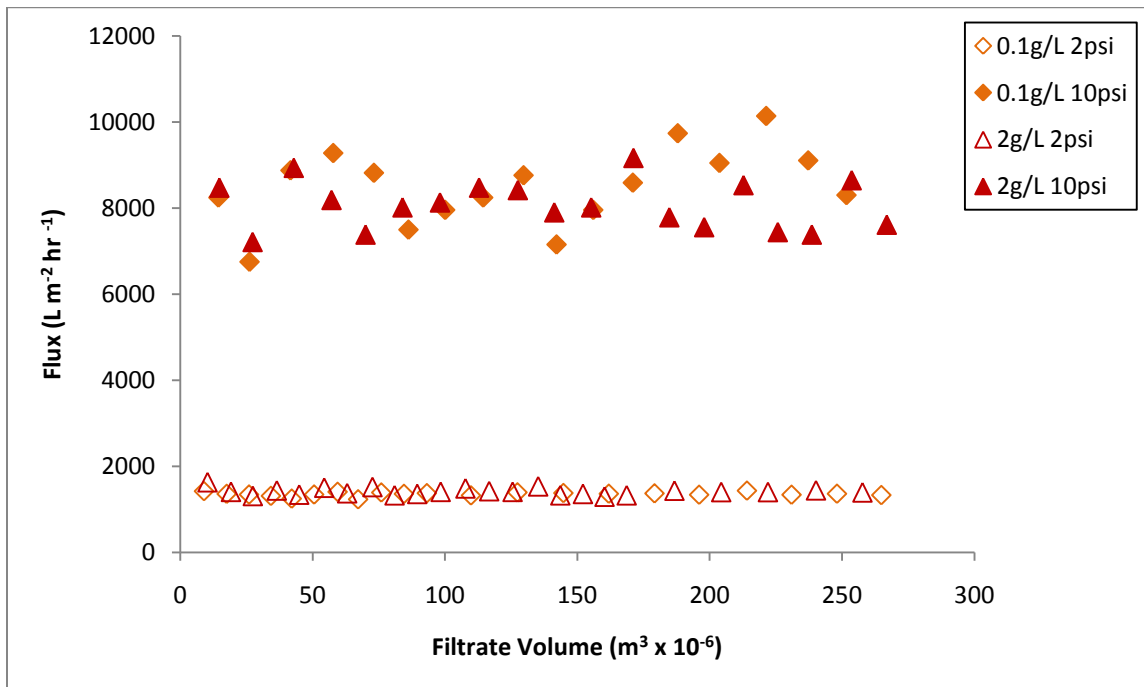

Figure 13: β-lactoglobulin permeate flux versus filtrate volume determined by filtering through 0.45 μm uncoated PTFE membrane. β-lactoglobulin solutions were prepared at pH 5.8 and operated at 2 psi and 10 psi. β-lactoglobulin permeate concentration was 0.1 g/L and 2 g/L.

4.2.2 Protein Transmission

When filtering the protein solution, samples of the permeate where taken to test the protein transmission. The protein transmission helps to determine the effect that the membrane surface, type of protein, and operating condition may have in the overall experiment. The permeate concentration of ovalbumin, lysozyme, and β-lactoglobulin are shown in Figure 14, Figure 15, Figure 16, and Figure 17 . Only uncoated PTFE was experimented with at 0.1 g/L concentration for each of the proteins since there was no change in flux or concentration transmission at this level. For each protein at 0.1 g/L, the permeate concentration stays very constant at 0.1 g/L. For both uncoated PTFE and coated PTFE, when each protein is at concentration 2 g/L, the permeate concentration has some variation, but the values stay close to 2 g/L. There does not appear to be any decline in protein concentration over time for the uncoated PTFE.

For PVA coated PTFE, there is a slight decline in protein transmission for the ovalbumin solution at 2 g/L and feed pressure 10 psi due to fouling of the ovalbumin. It appears that the decrease begins at 100 mL of filtrate volume. This means that only 0.2 g of ovalbumin has passed through the membrane at this point. At 100 mL, this is where the fouling mechanism transitions to cake filtration based on Figure 9 shown previously and Figure 24 shown later in section 4.2.3.

It has been found that at the isoelectric point, the protein transmission is at the highest point [41] but will stay constant if the protein buildup is slow or only internal fouling occurs [18]. Another study found that the protein transmission remained constant when internal fouling occurred, but would decrease when external fouling took place [19]. This helps explain why the protein transmission decreased slightly for ovalbumin. In the later section on FESEM images, this helps reinforce the idea of external fouling with ovalbumin.
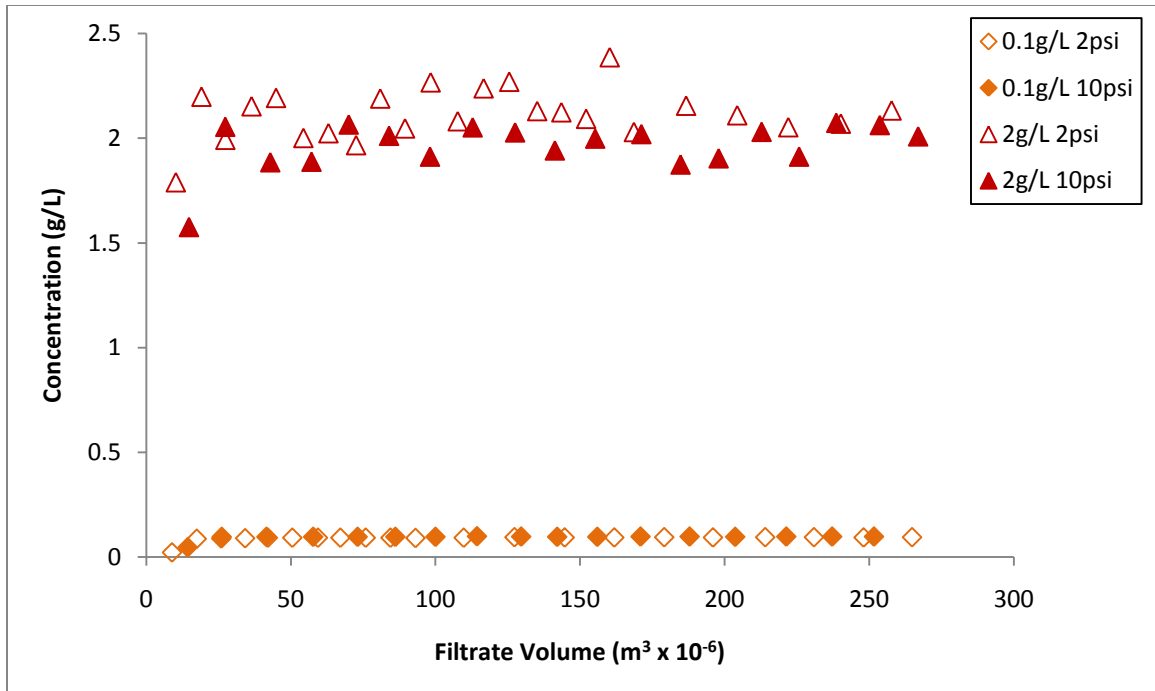
Figure 14: β-lactoglobulin permeate concentration versus filtrate volume determined by filtering through 0.45 µm uncoated PTFE membrane.
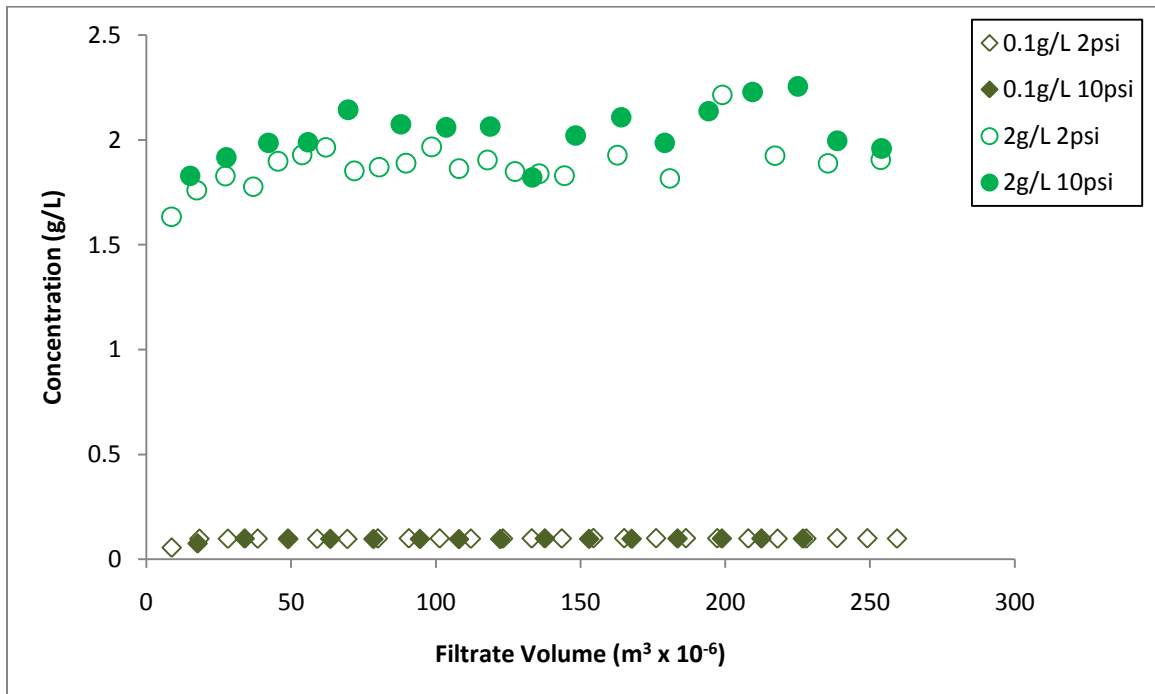

Figure 15: Lysozyme permeate concentration versus filtrate volume determined by filtering through 0.45 µm uncoated PTFE membrane.
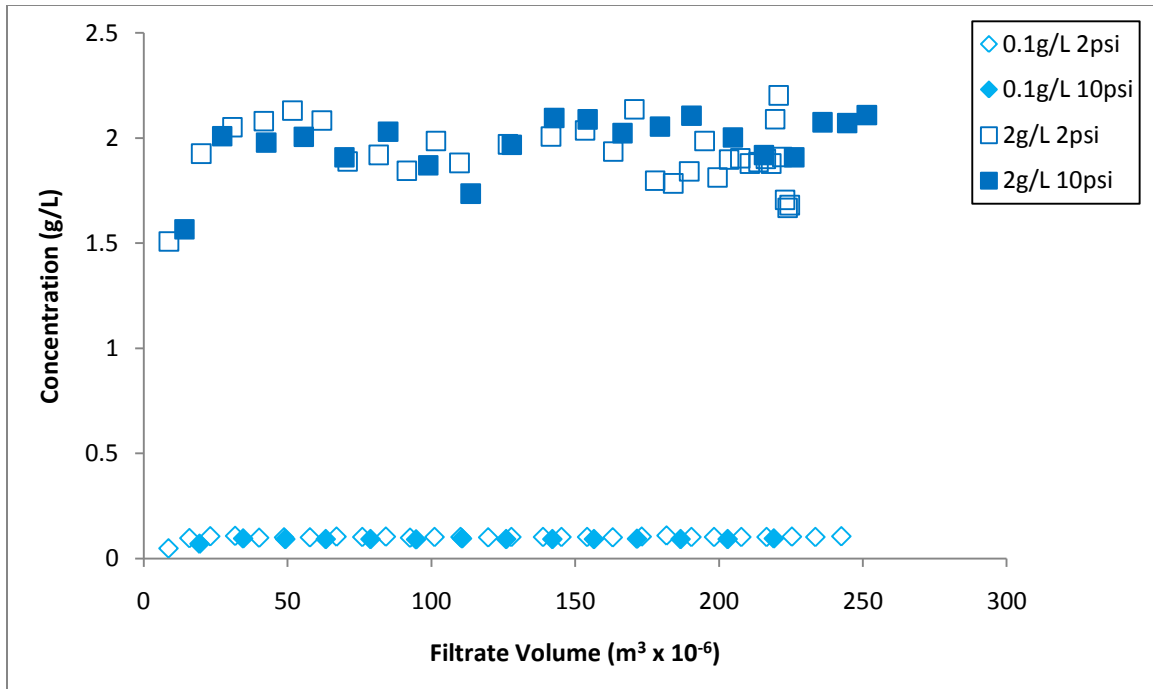
Figure 16: Ovalbumin permeate concentration versus filtrate volume determined by filtering through 0.45 μm uncoated PTFE membrane.
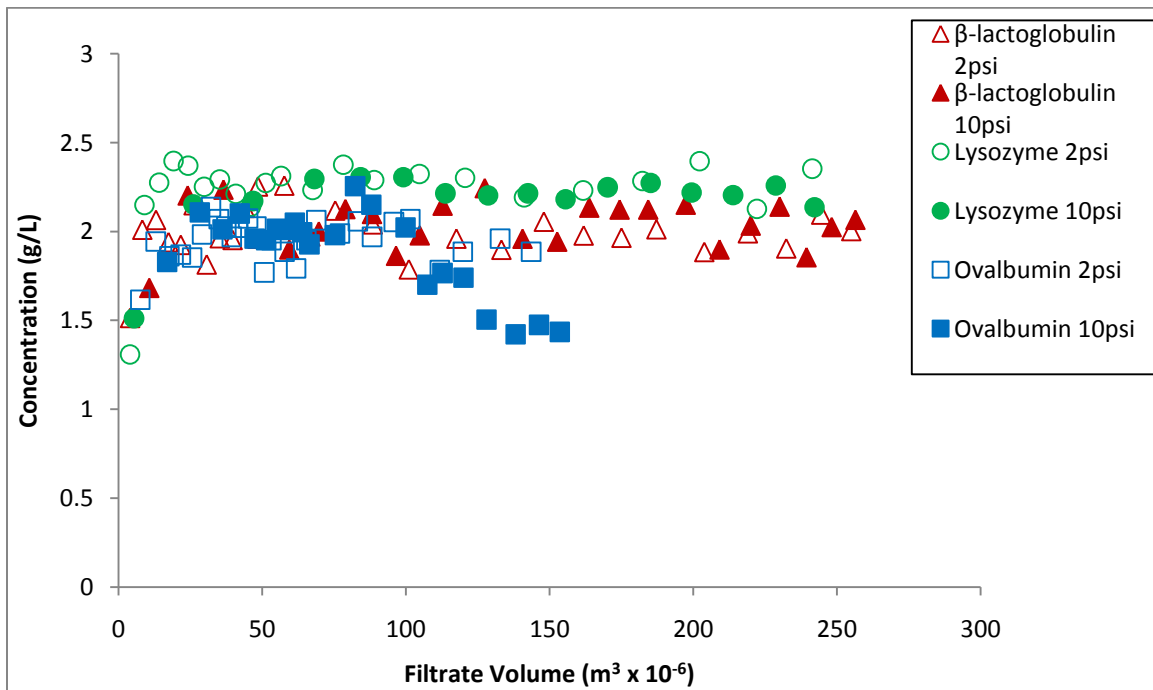

Figure 17: Each protein permeate concentration versus filtrate volume determined by filtering through 0.45 μm PVA coated PTFE membrane.

4.2.3. Membrane Surface Characterization

(i) Attenuated Total Reflection-Fourier Transform Infrared Spectroscopy (ATR-FTIR)

ATR-FTIR is a very useful analytical tool for surface characterization of membranes [43]. ATR-FTIR spectra for clean and fouled uncoated and PVA coated PTFE, is shown in both Figure 18 and Figure 19. From these figures there is a decrease in peak height at 1,100 and 1,300 cm^{-1} for the fouled membranes compared to clean PTFE. This is due to the protein deposited on the surface masking the chemical structure of the membrane. After pre-filtration, the peaks are higher than without pre-filtration of the protein solution. This would correspond to less protein being deposited on the surface. In these same figures shown below there is another graph that zooms in around wave numbers 1,480-1,780 cm^{-1}. By looking at the cleaned uncoated PTFE membrane there are no peaks present at 1,560 cm^{-1} and 1,650 cm^{-1} but when the membrane is fouled there are peaks present. This is related to the effect of protein being deposited which gives a larger peak. These peaks in this area correspond to amide bands I and II [37]. In particular amide I band corresponds to 1,650 cm^{-1} and amide II band is at 1,560cm^{-1}. Without any pre-filtration, these two peaks are larger due to proteins fouling the membrane. After pre-filtration there should be less aggregates leading to a lower degree of fouling and in turn this shows smaller peaks at 1,650cm^{-1} and 1,560cm^{-1}. Ovalbumin gives the highest peaks, which was expected from the flux data. The amide I band, usually between 1,600-1,700 cm^{-1}, is generally used for secondary structure analysis and originates from the C=O stretching vibration of the peptide groups [43]. In the lower 1600's the bands are normally due to β-sheets while the region around 1650 cm^{-1} is due to α-helices. The amide II band however is found in the 1,510 and 1,580 cm^{-1} region and is due to the bending of N-H groups and C-N stretching modes [43]. In particular, ovalbumin has α and β structures which help give amide I band at 1,639-1,655 cm^{-1} and an amide II band at 1,543 cm^{-1} [44].
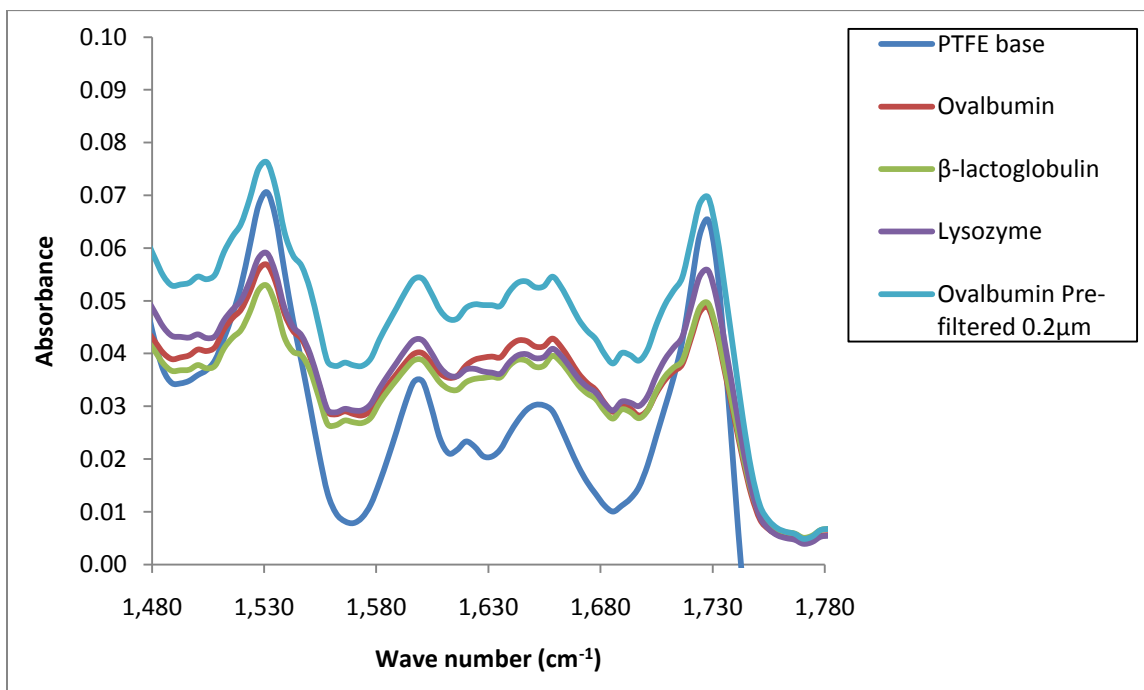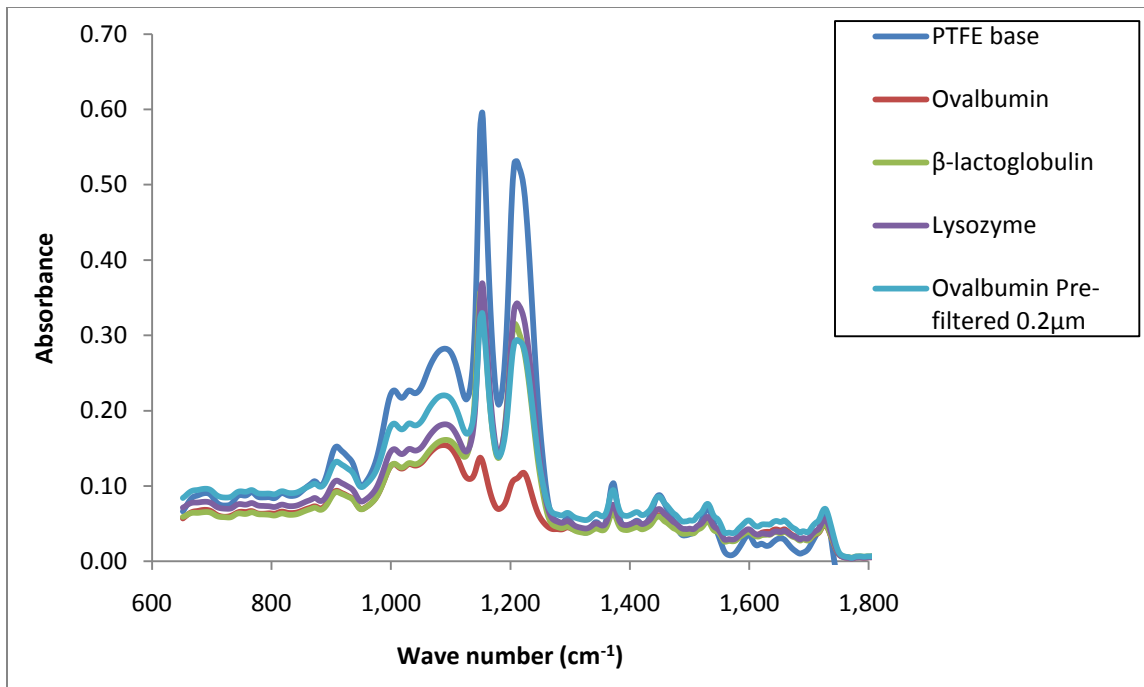
Figure 18: ATR-FTIR spectra for 0.45 µm uncoated PTFE membranes filtered with Ovalbumin, β-lactoglobulin, and lysozyme all operated at 10 psi and 2 g/L.
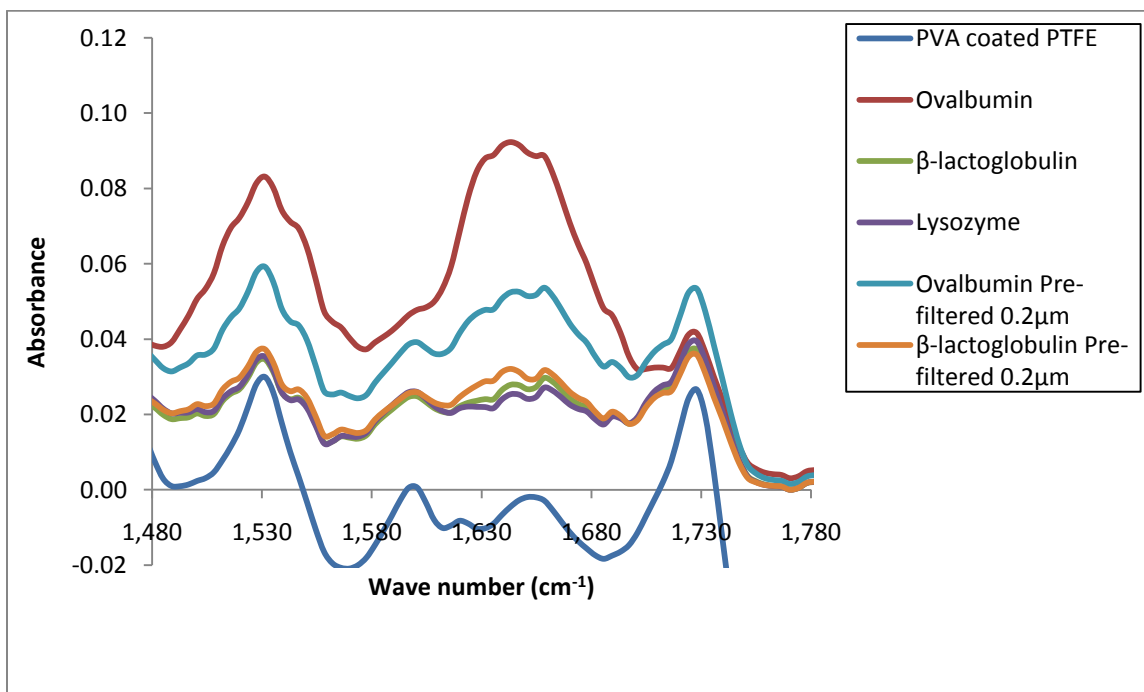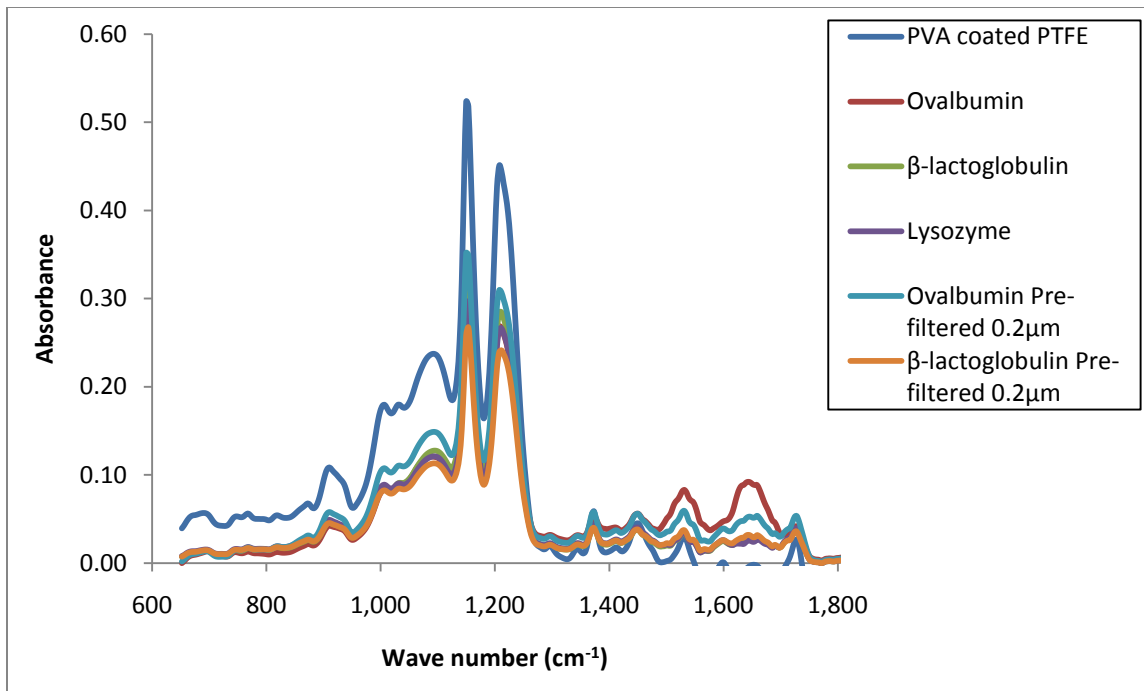
Figure 19: ATR-FTIR spectra for 0.45 µm PVA coated PTFE membranes filtered with Ovalbumin, β-lactoglobulin, and lysozyme all operated at 10 psi and 2 g/L.

*(ii) Field Emission Scanning Electron Microscopy (FESEM)*

FESEM images were taken of uncoated PTFE when the membrane was cleaned and fouled with the three separate proteins. Also images were taken of PVA coated PTFE when it was clean and fouled also with the three proteins. Each figure is at 2500x magnification for comparison. The cleaned uncoated PTFE membrane and the cleaned PVA coated PTFE membrane are shown in Figure 20 . From this figure, there are conspicuous pores that are interconnected for both the coated and uncoated PTFE. The FESEM figures of 2 g/L 10 psi for lysozyme, β-lactoglobulin, and ovalbumin fouled uncoated PTFE are shown in Figure 21 and for fouled PVA coated PTFE are shown in Figure 22 . These particular images are shown because they provide the highest conditions for fouling.

In Figure 21 of uncoated PTFE, lysozyme and β-lactoglobulin show a small degree of fouling but there are still distinct pores shown. However, for ovalbumin there is more fouling seen compared to the cleaned uncoated PTFE membrane. A few pores can still be seen but it appears that the membrane is heavily fouled by the ovalbumin. Each of the proteins were analyzed with the fouling mechanism prediction models. Only ovalbumin showed any significant fouling had occurred. From Figure 23 this confirms that the fouling mechanism of ovalbumin was the complete blocking of the pores.

The images of 2 g/L at 10 psi feed pressure of lysozyme, β-lactoglobulin, and ovalbumin filtered through PVA coated PTFE are shown in Figure 24. Lysozyme only shows a few areas that have some protein adsorption. β-lactoglobulin has more fouling occurring and less pores are noticable compared to the cleaned PVA coated PTFE membrane. Ovalbumin shows the greatest amount of fouling. There are no pores that can be seen and the adsorbed protein has formed a coating over the membrane. The mechanism of fouling for β-lactoglobulin and ovalbumin was determined using Equation 1 shown previously. These graphs are shown in Figure 23 and Figure 24. Based on these graphs β-lactoglobulin completely blocks the pores. In the case of uncoated

PTFE, ovalbumin completely blocks the pores, but for the PVA coated PTFE ovalbumin first appears to have a pore blockage method and then transitions into cake filtration over time. These results correspond to a study by Güell and Davis [18], which found that lysozyme had internal blocking and ovalbumin started with internal blocking and transitioned to cake filtration which completely blocks pores.

When comparing Figure 21 to Figure 22, it is clear that the fouled PVA coated PTFE membranes have much more protein deposition. Also when comparing the uncoated and PVA coated PTFE membranes in Figure 20, there are less pores visible when the membrane is coated with PVA.
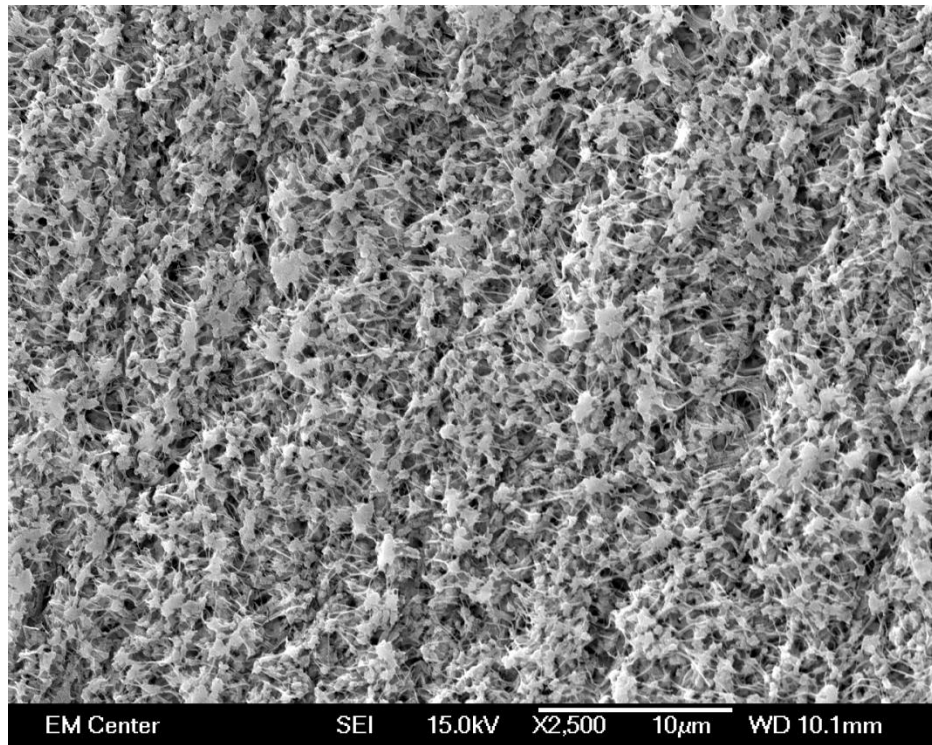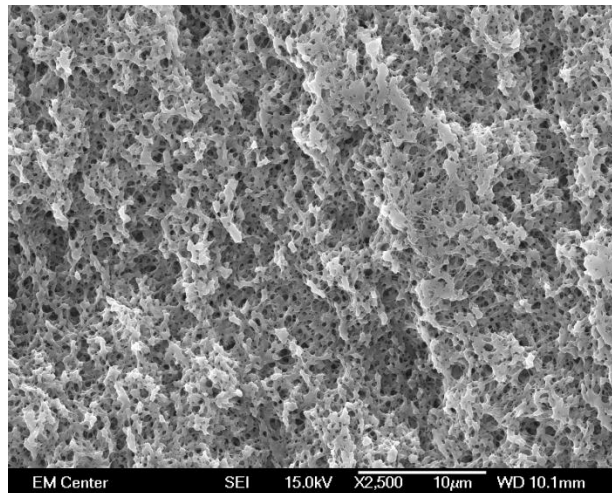
(a)
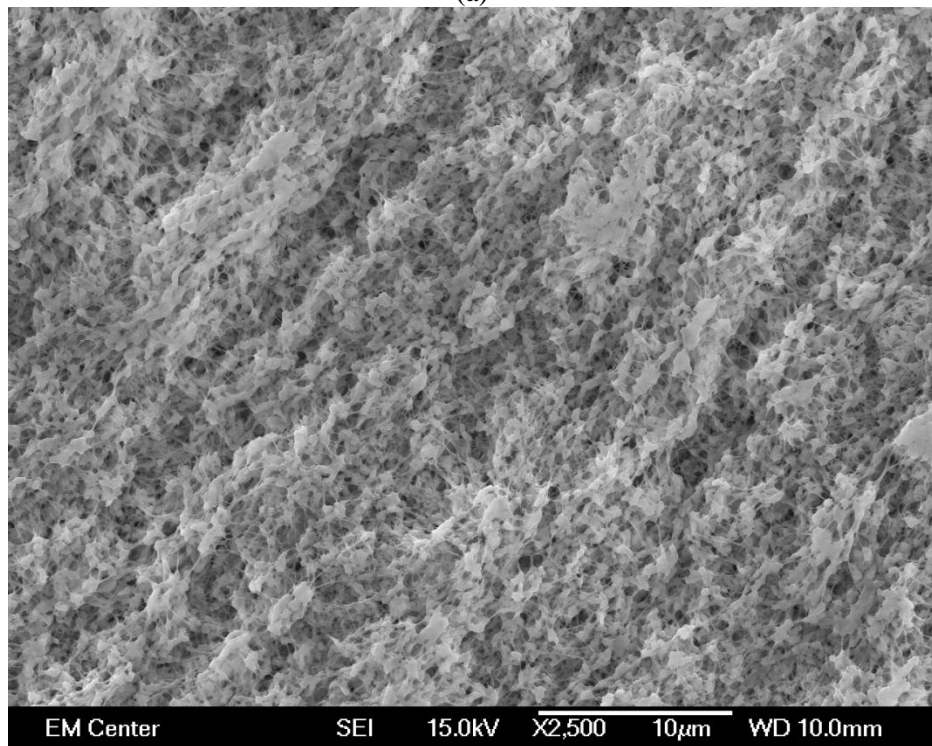
(b)

Figure 20: FESEM images of clean PTFE membranes with an effective pore size of 0.45 µm: (a) uncoated PTFE, (b) PVA coated PTFE.

(a)
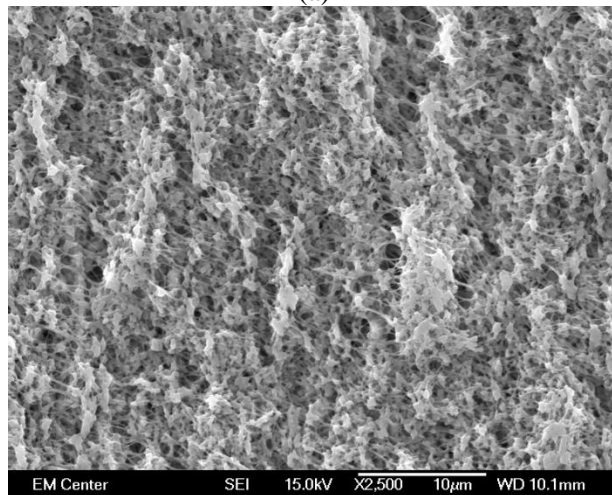
(b)
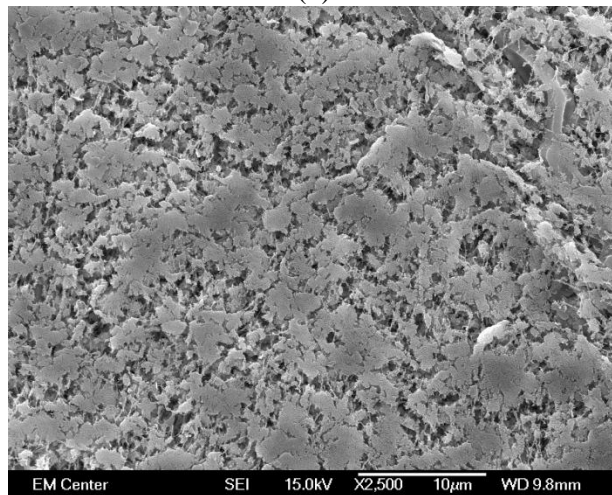
(c)

Figure 21: FESEM images of fouled 0.45 μm uncoated PTFE membranes: (a) 2 g/L β-lactoglobulin operated at 10 psi, (b) 2 g/L lysozyme operated at 10 psi, (c) 2 g/L ovalbumin operated at 10 psi.
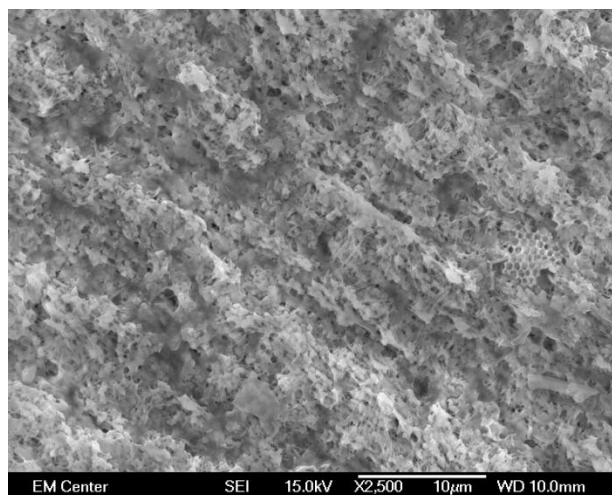
(a)
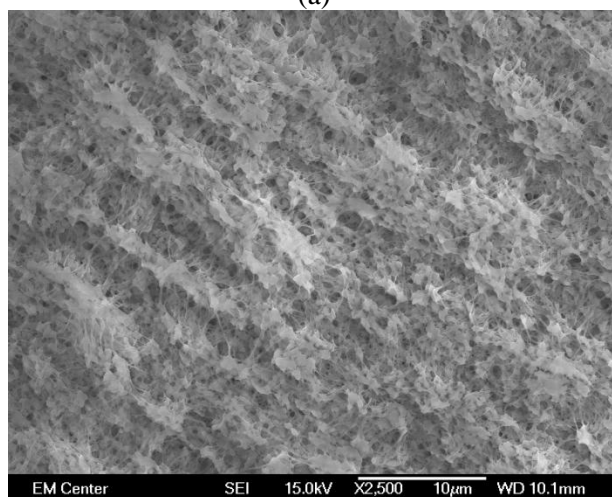
(b)
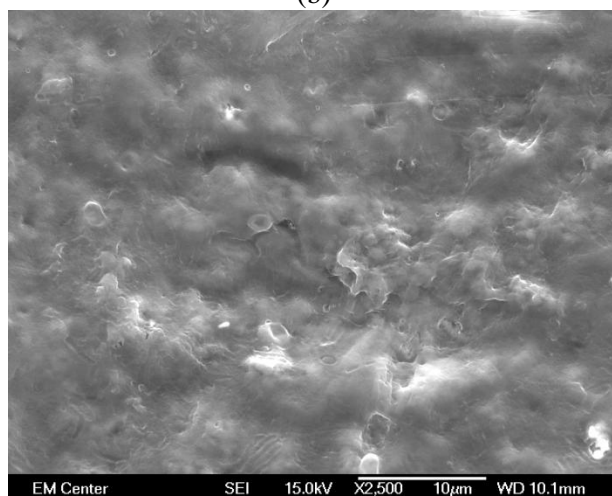
(c)

Figure 22: FESEM images of fouled 0.45 µm PVA coated PTFE membranes: (a) 2 g/L β-lactoglobulin operated at 10 psi, (b) 2 g/L lysozyme operated at 10 psi, (c) 2 g/L ovalbumin operated at 10 psi.

46
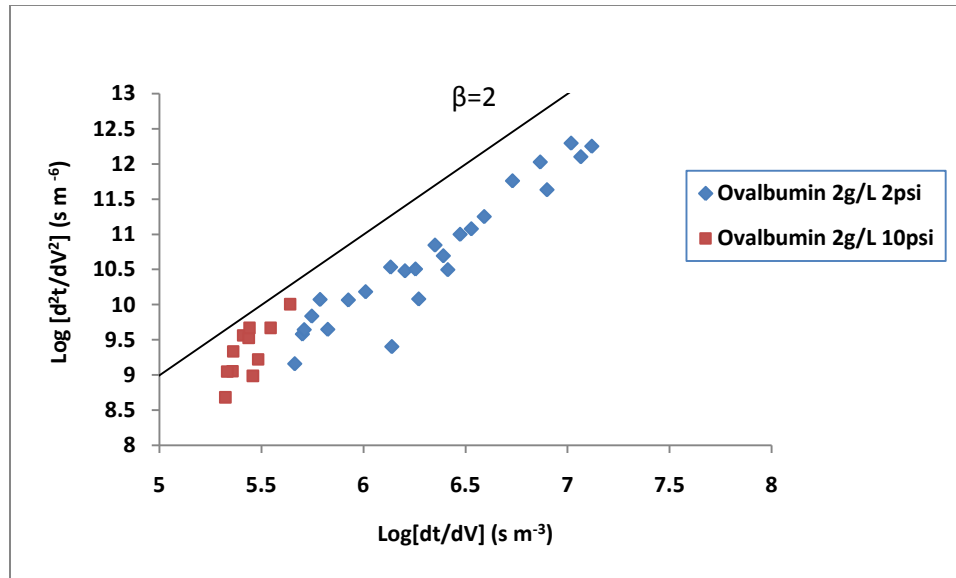
Figure 23: Fouling mechanism data when filtering ovalbumin at 2 g/L operated at 2 psi and 10 psi through 0.45 μm uncoated PTFE membrane.

Figure 24: Fouling mechanism data when filtering ovalbumin and β-lactoglobulin at 2 g/L operated at 2 psi and 10 psi through 0.45 μm PVA coated PTFE membrane.

4.3 UNCOATED PVDF & HYDROPHILIC COATED PVDF MEMBRANES

4.3.1. Protein Flux

(i) Effect of Type of Protein

The effect of lysozyme, β-lactoglobulin and ovalbumin on the permeate flux decline for uncoated PVDF membranes are shown in Figure 25 . Since the permeate flux for proteins at the concentration of 0.1 g/L at 2 psi and 10 psi was constant from previous experiments, only the results from proteins with a concen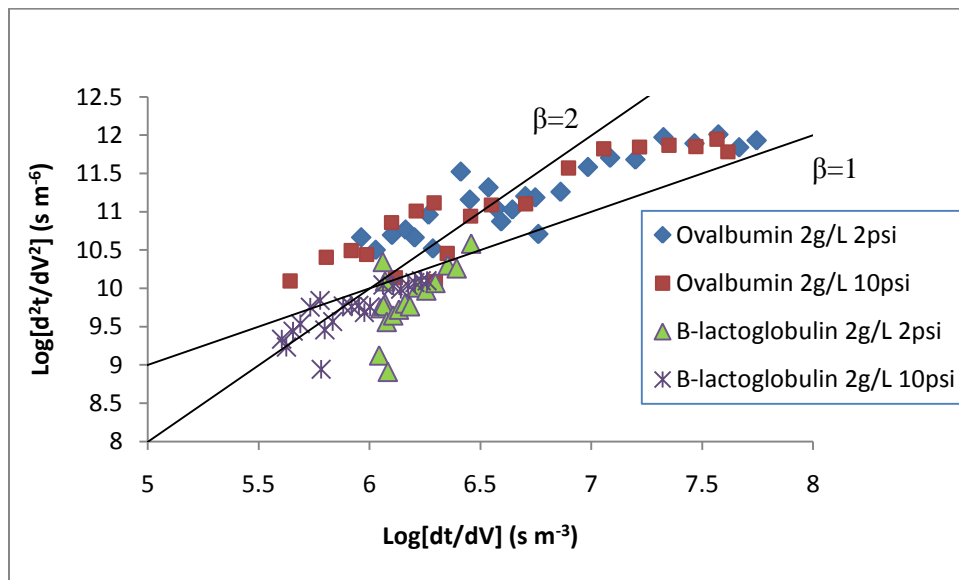tration of 2 g/L were included. The initial permeate flux for each of the proteins at the feed pressure of 2 psi is around 1,300 L/m^{2}hr. The initial permeate flux of each of the proteins for the high feed pressure of 10 psi is around 6,000-7,000 L/m^{2}hr. These values agree with the values of the phosphate buffer flux for uncoated PVDF. From this figure the only protein that may show a slight decrease in flux is ovalbumin at 10 psi. Since it does not appear to be a significant flux decline for any of the proteins, pre-filtration was not necessary.

Each of the three proteins were all filtered through PVA coated PVDF at 2 g/L 2 psi and 2 g/L 10 psi. Each of the different conditions is shown in Figure 26 . At 2 psi each of the proteins have a permeate flux that is initially about 1,100 L/m^{2}hr. At a feed pressure of 10 psi, the permeate flux is initially about 6,000-7,000 L/m^{2}hr. These values are consistent with permeate flux values for the phosphate buffer. At the feed pressure of 10 psi for ovalbumin solution there may be a slight decrease in flux as the permeate volume increases but it does not appear to be significant. This is similar to the uncoated PVDF. β-lactoglobulin and lysozyme, however, have constant fluxes at both low and high pressure as permeate volume increases. Since none of the proteins had significant flux declines, pre-filtration was not conducted.

Based on these figures, the hydrophobic and hydrophilic surfaces do not play much of a role. This has been shown to be the case in previous studies involving PVDF [45]. In this study there was very little fouling that occurred as well. Chen [45] determined that this was likely due to the high porosity so that any fouling occurring affects only a small percentage of the total pores.

Figure 25: Permeate flux versus filtrate volume determined by filtering through 0.45 μm uncoated PVDF membrane. Protein solutions were prepared at isoelectric pH for the protein and operated at 2 psi and 10 psi. The permeate concentration of the protein was 2 g/L.
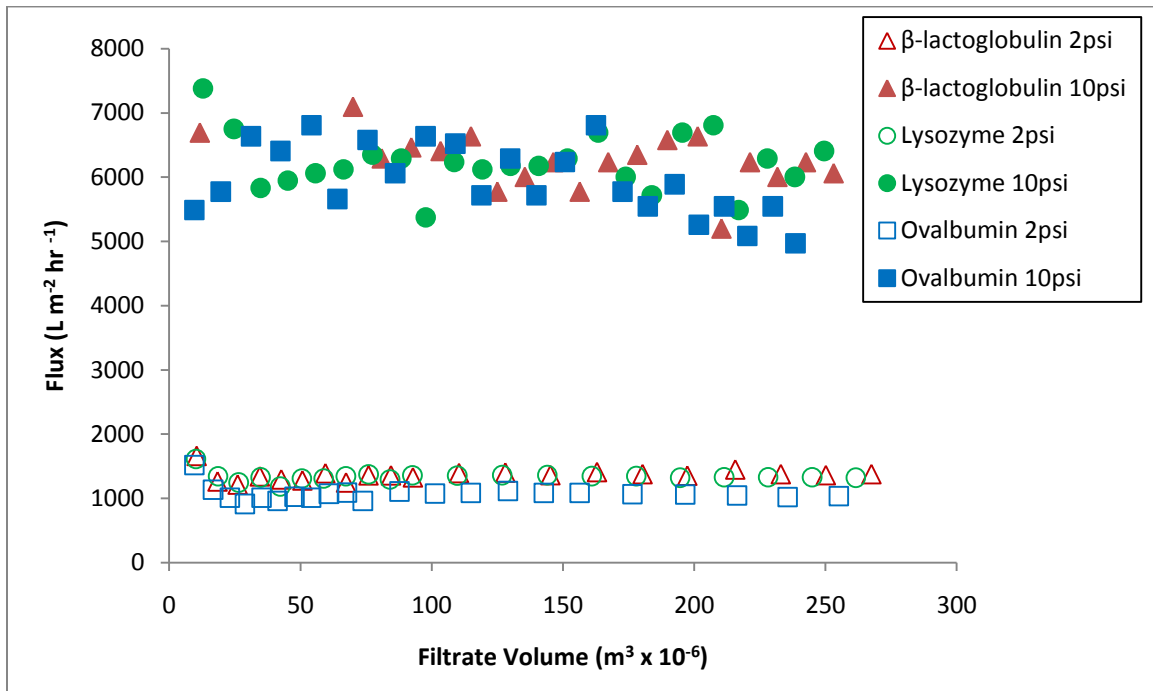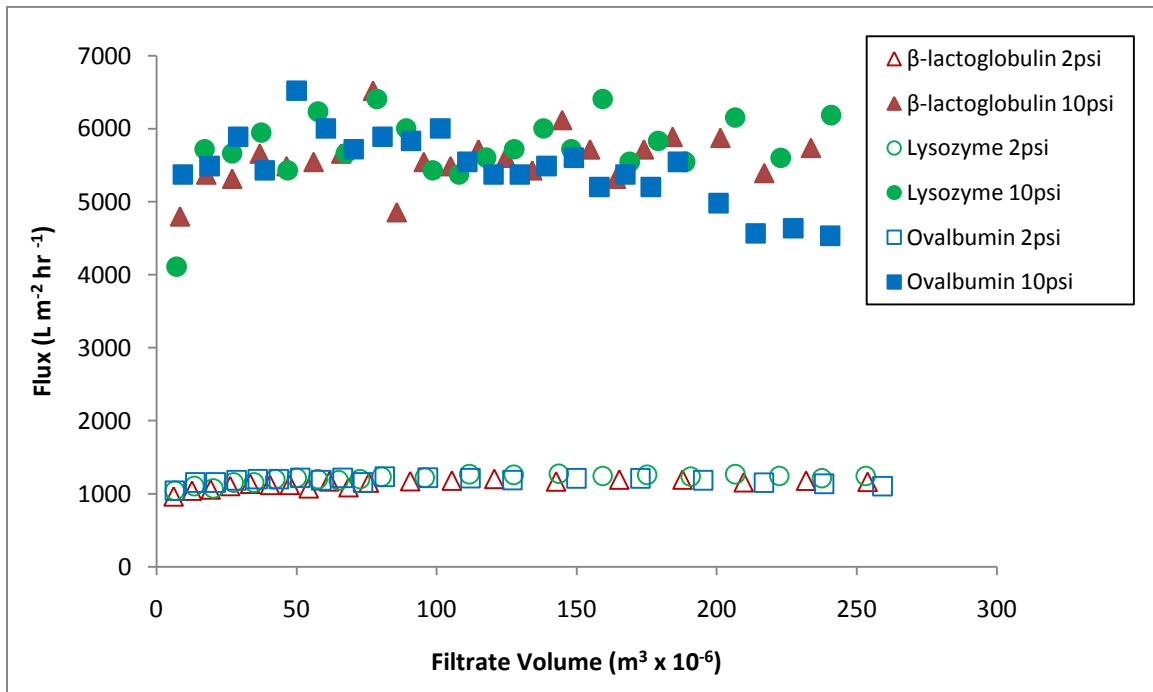

Figure 26: Permeate flux versus filtrate volume determined by filtering through 0.45 μm PVA coated PVDF membrane. Protein solutions were prepared at isoelectric pH for the protein and operated at 2 psi and 10 psi. The permeate concentration of the protein was 2 g/L.

(ii) Effect of Feed Pressure on Flux

The effect of feed pressure on permeate flux was shown in Figure 25 and Figure 26. The permeate flux of each protein and each membrane is lower when the feed pressure is at 2 psi and high when at 10 psi. This is the same trend as was seen with the phosphate buffer flux. When the feed pressure is 10 psi, the average permeate flux was around 6,000 L/m^{2}hr. This value was a little higher for uncoated PVDF and a little lower for coated PVDF which was seen for the PTFE membranes. When the feed pressure is 2 psi, the average permeate flux was just a little over 1,000 L/m^{2}hr.

4.3.2. Protein Transmission

Samples of the permeate fluid were taken to test the protein transmission. The permeate fluid concentration of ovalbumin, lysozyme, and β-lactoglobulin are shown in Figure 27 and Figure 28. For both the uncoated PVDF and PVA coated PVDF, the permeate concentration has some variation, but the values stay close to 2 g/L. There does not appear to be any decline in protein concentration over time for both membranes which was seen previously with the PTFE membranes.

Figure 27: Permeate concentration versus filtrate volume determined by filtering through 0.45 μm uncoated PVDF membrane. Protein solutions were prepared at isoelectric pH for the protein and operated at 2 psi and 10 psi. The permeate concentration of the protein was 2 g/L.
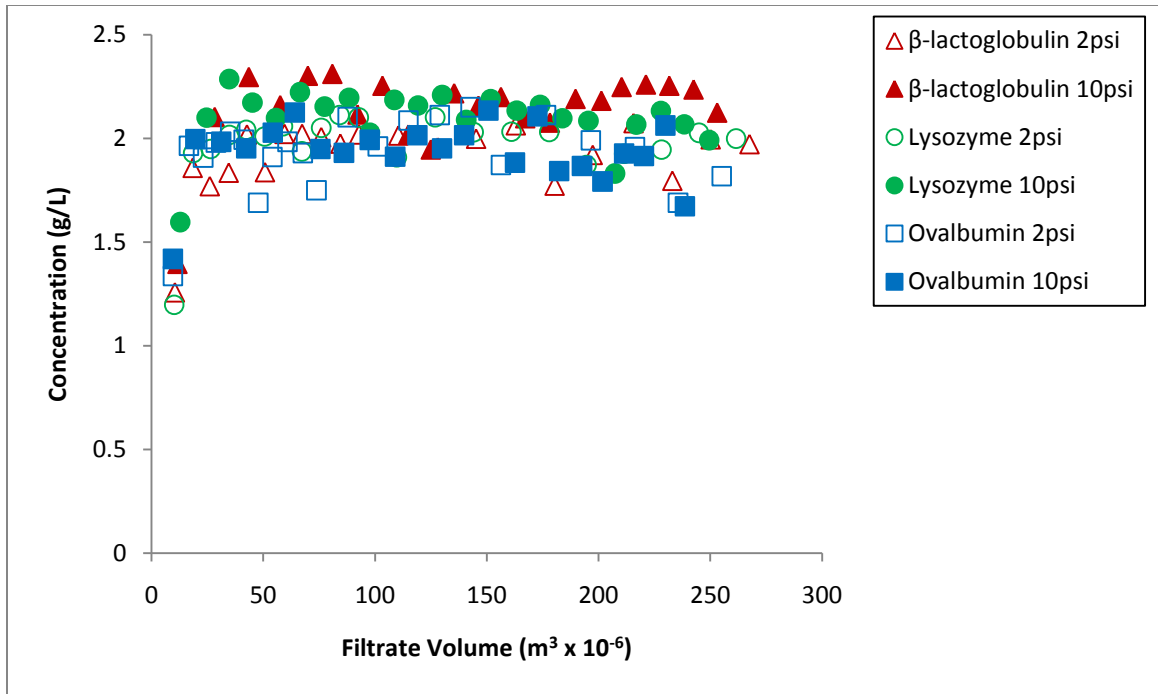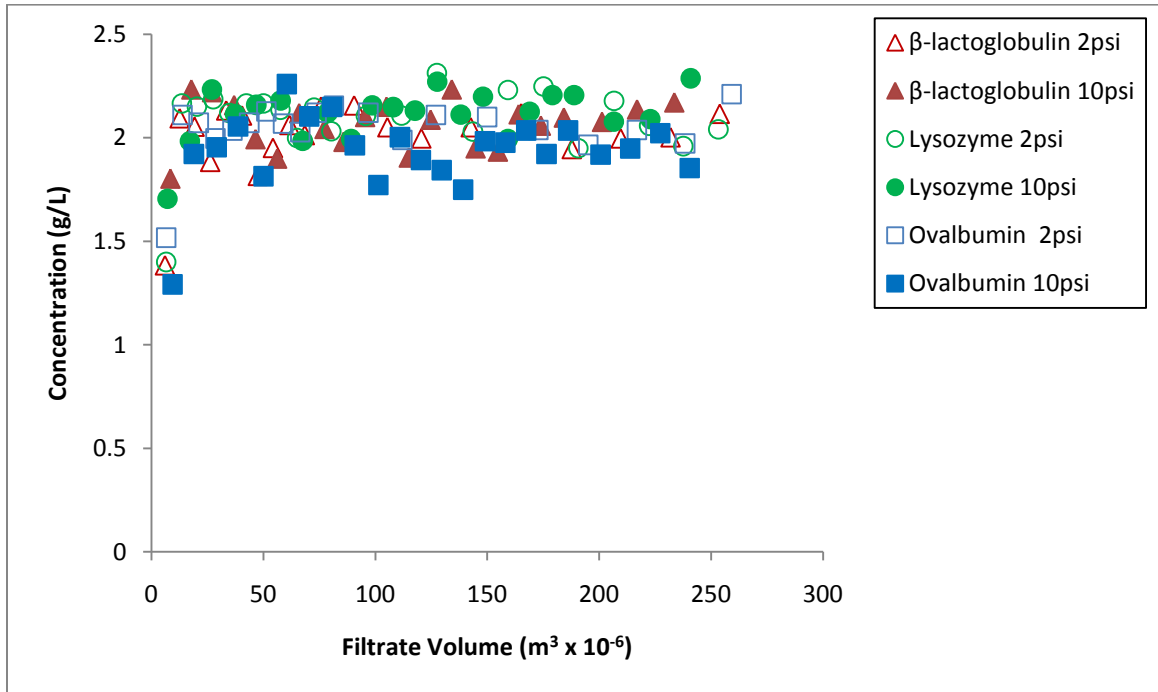

Figure 28: Permeate concentration versus filtrate volume determined by filtering through 0.45 μm PVA coated PVDF membrane. Protein solutions were prepared at isoelectric pH for the protein and operated at 2 psi and 10 psi. The permeate concentration of the protein was 2 g/L.

4.3.3. Membrane Surface Characterization

(i) Attenuated Total Reflection-Fourier Transform Infrared Spectroscopy (ATR-FTIR)

One method to characterize the membrane surface is using Attenuated Total Reflectance Fourier Transform Infrared Spectroscopy. PVDF is known to have a fairly simple structure of ($-CH_2-CF_2-$) which can help give the structure flexibility and some stereochemical constraint [24].

ATR-FTIR spectra for clean and fouled uncoated and PVA coated PVDF, is shown in Figure 29 and Figure 30. C-F stretching peaks can normally be found at 1,150 and 1,210 cm^{-1} [24] but from these graphs the peaks seem to be shifted slightly to the left with peaks at 1,075 and 1,190 cm^{-1}. From these figures there is just a slight decrease in peak height around 1,190 cm^{-1} for the fouled membranes compared to clean PVDF. Since this is such a minor decrease, this corresponds to very little protein deposited on the membrane surface so that the chemical structure of the membrane still dominates. However, the peak around 1,075 cm^{-1} for both uncoated PVDF and PVA coated PVDF shows a decline after fouling has occurred with the proteins.

These figures are zoomed in around wave numbers 1,480-1,780 cm^{-1}. By looking at the cleaned PVDF membranes there are peaks present around 1,560 cm^{-1} and 1,650 cm^{-1} but when the membrane is fouled the peaks are more prominent due to protein deposition. These peaks in these two areas correspond to amide bands I around 1,650 cm^{-1} and amide band II around 1,560cm^{-1} [37]. Each of the proteins appear to have some deposition occurring on the membrane.
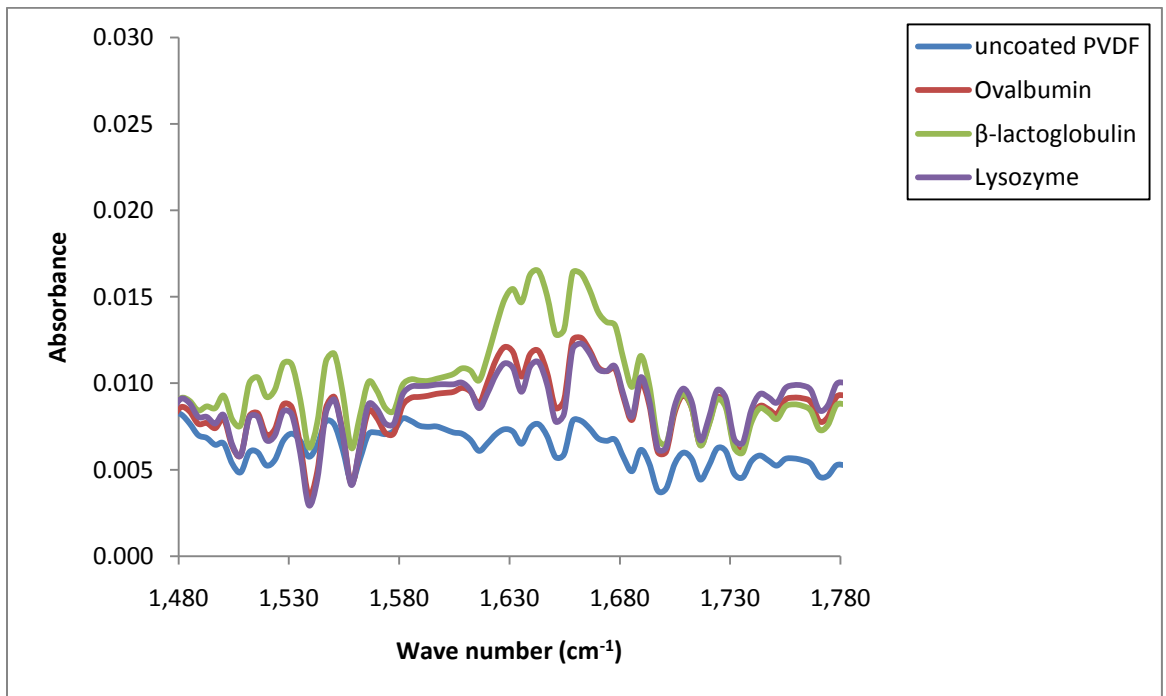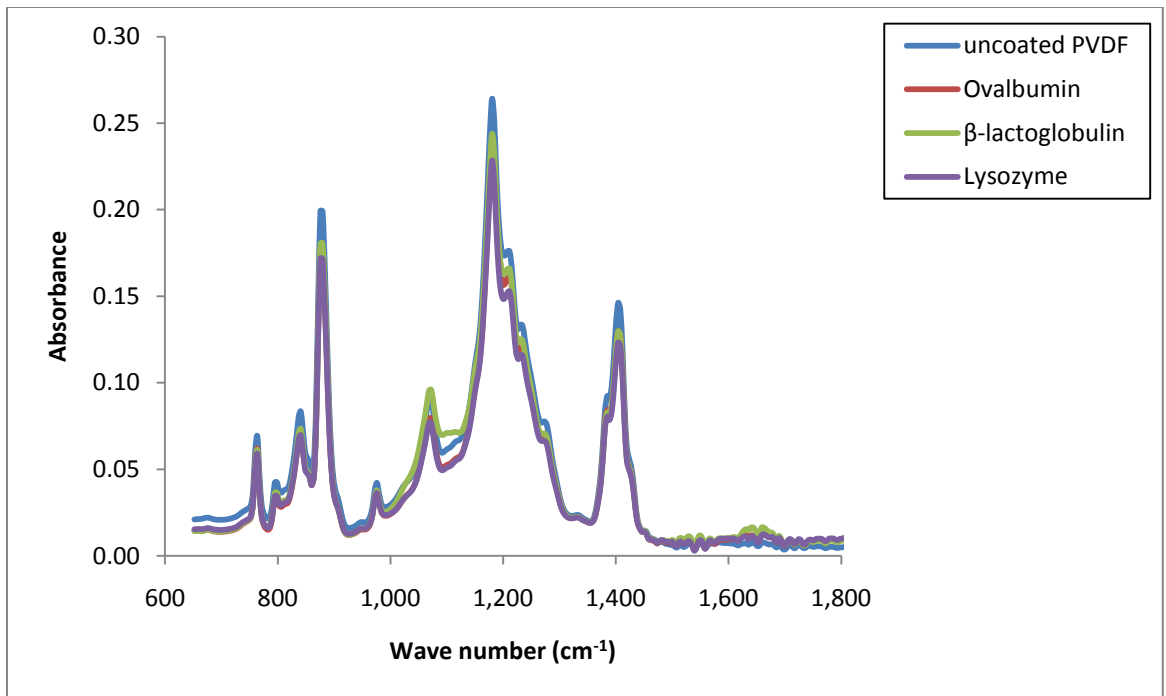
Figure 29: ATR-FTIR spectra for 0.45 μm uncoated PVDF membranes filtered with ovalbumin, β-lactoglobulin, and lysozyme all operated at 10 psi and 2 g/L.
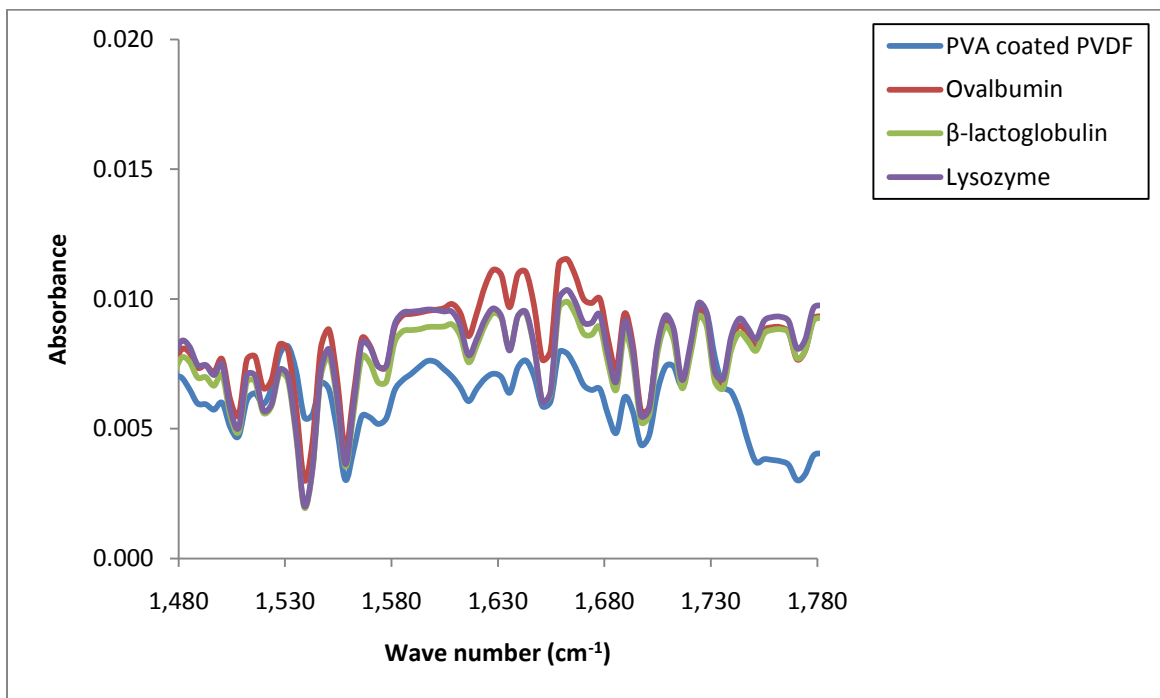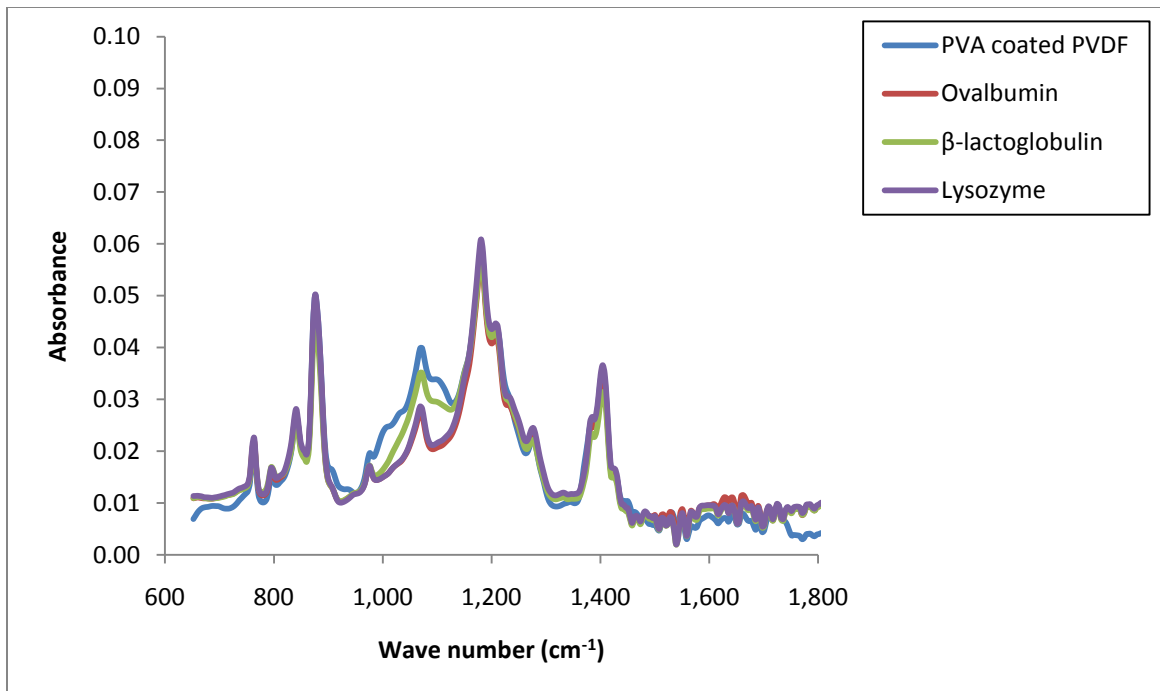
Figure 30: ATR-FTIR spectra for 0.45 µm PVA coated PVDF membranes filtered with β-lactoglobulin, ovalbumin, and lysozyme all operated at 10 psi and 2 g/L.
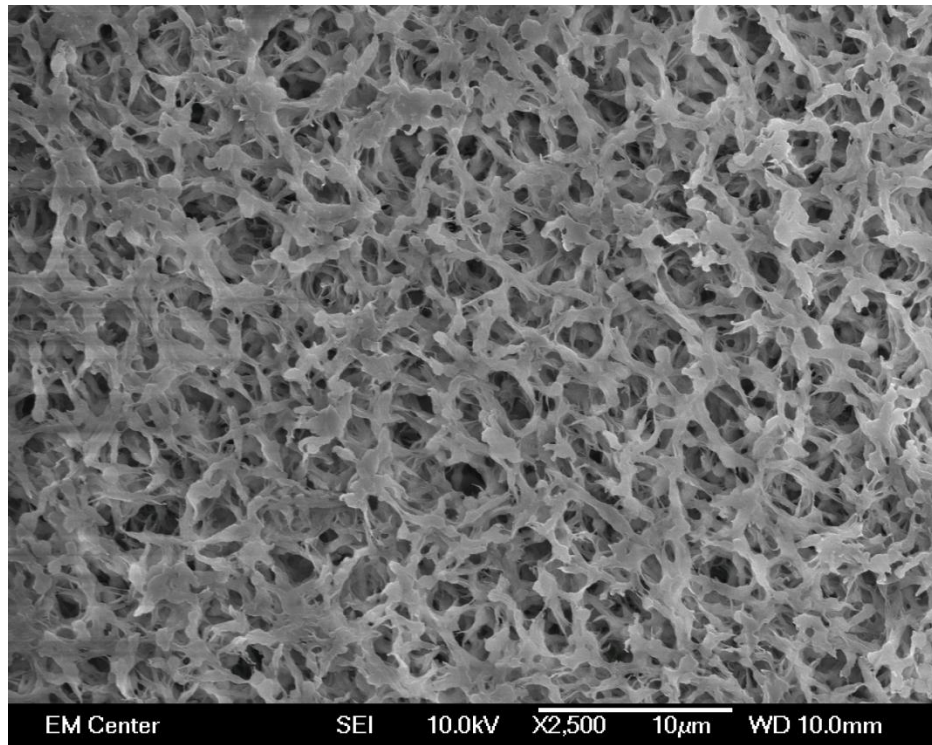
(ii) Field Emission Scanning Electron Microscopy (FESEM)

FESEM images were taken of uncoated and PVA coated PVDF when the membrane was cleaned and fouled with the three separate proteins. Each image was taken at 2500x magnification for comparison purposes. The cleaned uncoated PVDF membrane and the cleaned PVA coated PVDF membrane are shown in Figure 31. From these images, there are clearly pores that are interconnected. The FESEM figures of lysozyme, β-lactoglobulin, and ovalbumin, operated at 2 g/L 10 psi, for fouled uncoated PVDF are shown in Figure 32 and for fouled PVA coated PVDF are shown in Figure 33. These images were choosen to present the highest conditions for fouling.

In Figure 32 lysozyme and β-lactoglobulin do not show any noticable fouling. All of the pores can still be seen. However, for ovalbumin there is more fouling seen compared to the cleaned uncoated PVDF membrane. Although there is aggregation of ovalbumin on the membrane surface, most of the pores can still be seen.

In Figure 33 lysozyme, and β-lactoglobulin show a small degree of fouling with areas of aggregated protein but there are still distinct pores that can be seen. However, for ovalbumin there is more fouling seen compared to the cleaned PVA coated PVDF membrane. The membrane pores can still be seen but it appears that the membrane is more heavily fouled by the ovalbumin than lysozyme, and β-lactoglobulin.

When comparing 2 g/L at 10 psi feed pressure of lysozyme, β-lactoglobulin, and ovalbumin filtered through PVA coated PVDF to filtering the proteins through uncoated PVDF, there is more fouling present in the PVA coated PVDF membranes based on Figure 32 and Figure 33.

EM Center   SEI   10.0kV   X2,500   10μm   WD 10.0mm

(a)

EM Center   SEI   15.0kV   X2,500   10μm   WD 10.0mm
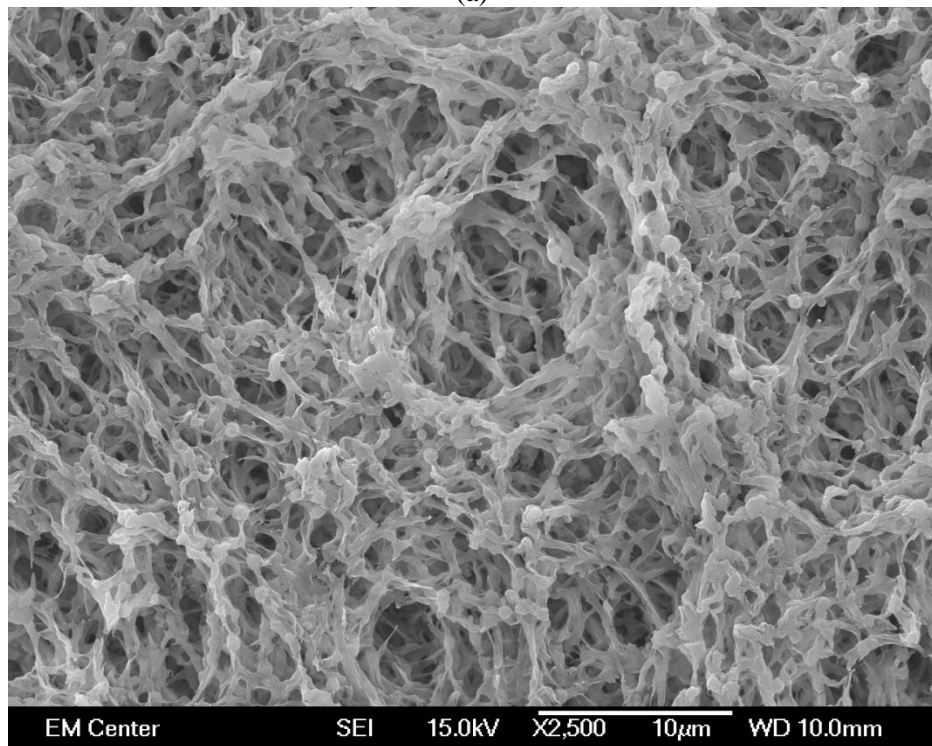
(b)

Figure 31: FESEM images of clean PVDF membranes with an effective pore size of 0.45 μm: (a) uncoated PVDF, (b) PVA coated PVDF.
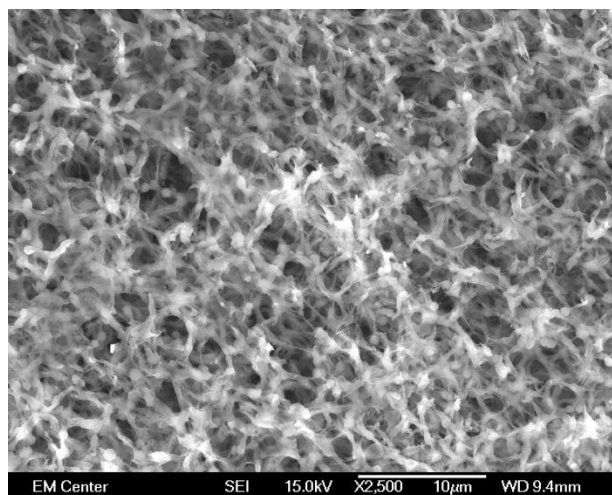
(a)
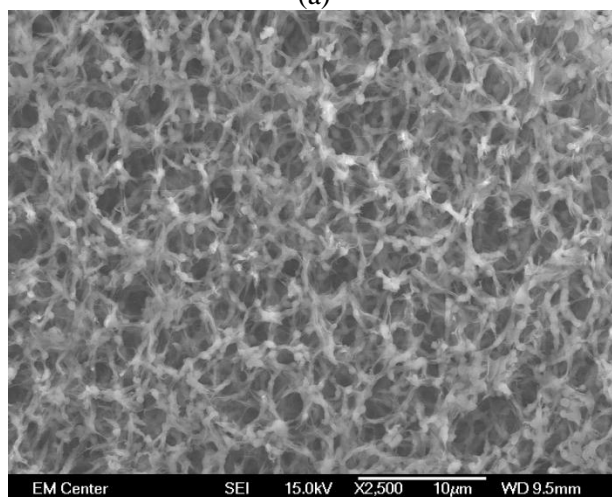
(b)
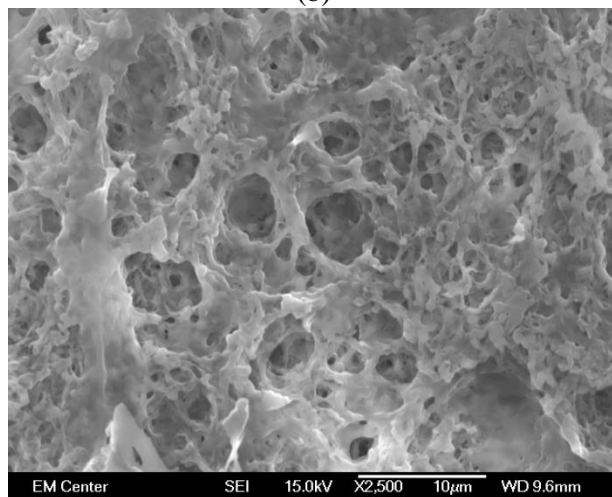
(c)

Figure 32: FESEM images of fouled 0.45 µm uncoated PVDF membranes: (a) 2 g/L β-lactoglobulin operated at 10 psi, (b) 2 g/L lysozyme operated at 10 psi, (c) 2 g/L ovalbumin operated at 10 psi.
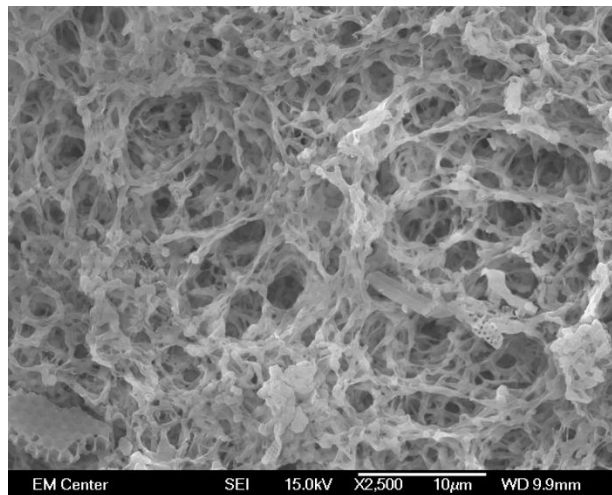
(a)
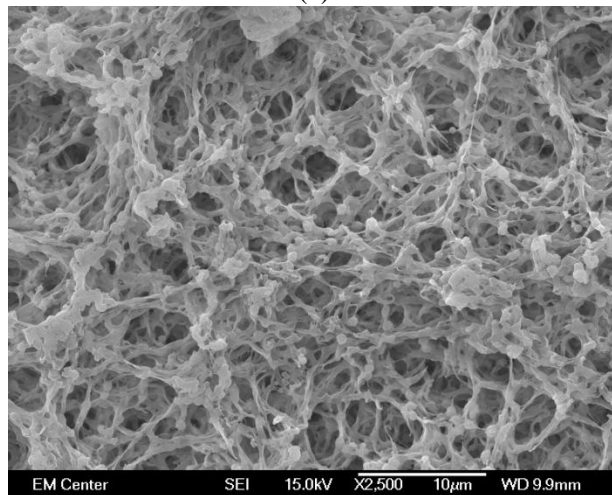
(b)
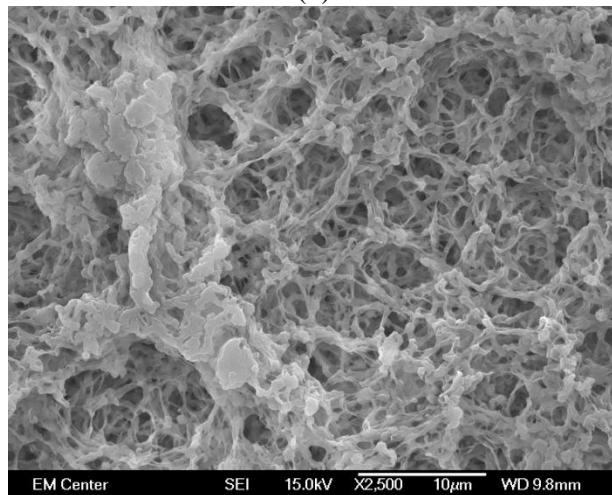
(c)

Figure 33: FESEM images of fouled 0.45 µm PVA coated PVDF membranes: (a) 2 g/L β-lactoglobulin operated at 10 psi, (b) 2 g/L lysozyme operated at 10 psi, (c) 2 g/L ovalbumin operated at 10 psi.

4.4 PTFE VERSUS PVDF MEMBRANE

Based on the data gathered from the permeate flux, ATR-FTIR graphs, and FESEM images there is quite a bit of difference between PTFE and PVDF membranes. Even though each of the membranes contained pores 0.45 μm in diameter, they produced different results based on surface chemistry and morphology.

One study found that PVDF had the lowest flux reduction of the hydrophobic membranes they tested [22]. This agrees with the findings shown above. PTFE membranes tend to have a more significant change in flux for both PVA coated and uncoated than for the PVDF membranes.

Another study tested CA, nylon-66, hydrophobic PVDF, and hydrophilic PVDF and found that the hydrophilic PVDF had the lowest amount of protein adsorption [42]. This correlates with the differences shown between PTFE and PVDF.

CHAPTER 5. CONCLUSIONS

From the experimental results, a significant flux decline was seen for ovalbumin at 2 g/L both low and high pressures when filtering through the 0.45 μm uncoated PTFE membrane. For the 0.45 μm PVA coated PTFE membrane, both ovalbumin and β-lactoglobulin showed a severe decrease in flux at 2 g/L and both pressures. By using protein solutions at their corresponding isoelectric points it was expected to have the greatest amount of aggregation since the electric charge is neutralized [40]. These findings were supported by FESEM figures, ATR-FTIR data, flux graphs, and fouling mechanism models. For the uncoated PTFE membrane, ovalbumin demonstrated a complete blocking mechanism where the solute completely blocked the pores. For the PVA coated PTFE membranes, however, β-lactoglobulin exhibited a complete blocking mechanism, while ovalbumin showed multiple mechanisms of blockage. Ovalbumin appeared to begin fouling be a pore blockage mechanism and then it transitioned to a cake filtration mechanism. Overall, ovalbumin showed the most flux decline and highest degree of fouling, β-lactoglobulin showed the next greatest decrease in flux, and lysozyme showed no flux decline with only a slight buildup of protein on the membrane.

Uncoated and PVA coated PVDF membranes were quite different from the PTFE membranes. Based on the flux data, FESEM images and the ATR-FTIR figures, each of the three proteins had minimal fouling and no significant decrease in flux. Only the FESEM figures helped distinguish the differences between the proteins. While this was only a qualitative result and the images could vary based on location on the membrane, ovalbumin had the highest degree of aggregates deposited on the membrane, with β-lactoglobulin showing slightly more protein fouling than lysozyme. Kelly and Zydney [49] had found that these aggregates in the solution are

quite large since they can block pores and for microfiltration the pores sizes are relatively large. This also agrees with other findings that have shown that ovalbumin has the most aggregates in solution and this leads to a large flux decline [18]. Also these findings are confirmed by another study that showed lysozyme having the smallest amount of flux decline, while ovalbumin and β-lactoglobulin both had severe flux declines [2].

Overall many different properties were shown to affect the amount of flux decline. The type of protein, isoelectric point of the protein, protein concentration, membrane morphology, surface chemistry of the membrane, feed pressure, and protein aggregation all play a role in the mechanism of protein fouling. Since there can be so many variables in the process, filtering proteins is a complicated process. Better surface characterization methods and models to determine the fouling mechanism are needed to gain a better understanding of using microfiltration membranes for filtering protein solutions.

CHAPTER 6. FUTURE STUDIES

1. It would be useful to use quasi-elastic light scattering to help determine if there are aggregates in the protein solution. This would be helpful to better characterize protein fouling. Knowing the amount of aggregates and how large the aggregates become would further the understanding of protein fouling and help determine appropriate pre-filtration membrane pore size.

2. Along with understanding more about aggregates in solution, it would be helpful to determine if the proteins are becoming denatured or are in their native structure throughout the experiment.

3. Since the PVA coated membranes were hydrophilic but resulted in a greater flux decline than hydrophobic membranes, it would be useful to have membranes that have a different type of hydrophilic coating. This would provide a comparison to determine how the PVA coating is affecting the amount of fouling.

4. All of the experiments were run in dead end filtration mode and it would be useful to run experiments with tangential flow filtration. This would be beneficial to increase the understanding of why flux declines when proteins are present in solution. This would include shear induced by fluid feed flow.

REFERENCES

[1] C. Duclos-Orsello, W. Li, C. Ho, A Three Mechanism Model to Describe Fouling of Microfiltration Membranes, Journal of Membrane Science, 280 (2006) 856–866.

[2] S.T. Kelly, A.L. Zydney, Protein Fouling During Microfiltration: Comparative Behavior of Different Model Proteins, Biotechnology and Bioengineering, 55 (1997) 91-100.

[3] R. Chan, V. Chen, Characterization of Protein Fouling on Membranes: Opportunities and Challenges, Journal of Membrane Science, 242 (2004) 169-188.

[4] M. Mulder, Basic Principles of Membrane Technology, 2nd Ed., Kluwer Academic Publishers, USA, 1996.

[5] R.W. Baker, Membrane Technology and Applications, 2nd Ed., John Wiley & Sons, Inc., USA, 2004.

[6] Membrane Handbook, W.S.W. Ho, K.K. Sirkar (Eds), Kluwer Academic Publishers, USA, 1992.

[7] R. van Reis, A. Zydney, Review: Bioprocess Membrane Technology, Journal of Membrane Science 297 (2007) 16–50.

[8] D.M. Kanani, X. Sun, R. Ghosh, Reversible and Irreversible Membrane Fouling during In-line Microfiltration of Concentrated Protein Solutions, Journal of Membrane Science, 315 (2008) 1-10.

[9] J. Zhang, Z. Cai, W. Cong, Z. Su, F. Ouyang, Mechanisms of Protein Fouling in Microfiltration. I. Determination of Proteins Fouled on Microfiltration Membranes, Separation Science and Technology, 37 (2002) 3025-3038.

[10] J. Zhang, Z. Cai, W. Cong, Z. Su, F. Ouyang, Mechanisms of Protein Fouling in Microfiltration. II. Adsorption and Deposition of Proteins on Microfiltration Membranes, Separation Science and Technology, 37 (2002) 3039-3051.

[11] F. Martinez, A. Martin, P. Pradanos, J.I. Calvo, L. Palacio, A. Hernandez, Protein Adsorption and Deposition onto Microfiltration Membranes: The Role of Solute–Solid Interactions, Journal of Colloid and Interface Science, 221 (2000) 254-261.

[12] S.T. Loh, U. Beuscher, T.K. Poddar, A.G. Porter, J.M. Wingard, S.M. Husson, S.R. Wickramasinghe, Interplay Among Membrane Properties, Protein Properties and Operating

Conditions on Protein Fouling during Normal-flow Microfiltration, Journal of Membrane Science, 332 (2009) 93-103.

[13] S.P. Palecek, A.L. Zydney, Hydraulic Permeability of Protein Deposits Formed during Microfiltration: Effect of Solution pH and Ionic Strength, Journal of Membrane Science, 95 (1994) 71-81.

[14] C. Velasco, M. Ouammou, J.I. Calvo, A. Hernández, Protein Fouling in Microfiltration: Deposition Mechanism as a Function of Pressure for Different pH, Journal of Colloid and Interface Science, 266 (2006) 148-152.

[15] S.P. Palecek, A.L. Zydney, Intermolecular Electrostatic Interaction and Their Effect on Flux and Protein Deposition during Protein Filtration, Biotechnology Progress, 10 (1994) 207-213.

[16] K.-L. Tunga, Y.-L. Li, S. Wang, D. Nanda, C.-C. Hu, C.-L. Li, J.-Y.Lai, J. Huang, Performance and Effects of Polymeric Membranes on the Dead-end Microfiltration of Protein Solution during Filtration Cycles, Journal of Membrane Science, 352 (2010) 143-152.

[17] E.M. Tracey, R.H. Davis, Protein Fouling of Track-Etched Polycarbonate Microfiltration Membranes, Journal of Colloid and Interface Science, 167 (1994) 104-116.

[18] C. Güell, R.H. Davis, Membrane Fouling during Microfiltration of Protein Mixtures, Journal of Membrane Science, 119 (1996) 269-284.

[19] J. Mueller, R.H. Davis, Protein Fouling of Surface-Modified Polymeric Microfiltration Membranes, Journal of Membrane Science, 116 (1996) 47-60.

[20] S.T. Kelly, W.S. Opong, A.L. Zydney, The Influence of Protein Aggregates on the Fouling of Microfiltration membranes during Stirred Cell Filtration, Journal of Membrane Science, 80 (1993) 175-187.

[21] N. Maximous, G. Nakhla, W. Wan, Comparative Assessment of Hydrophobic and Hydrophilic Membrane Fouling in Wastewater Applications, Journal of Membrane Science, 339 (2009) 93-99.

[22] C. Jönsson, A.-S. Jönsson, Influence of the Membrane Material on the Adsorptive Fouling of Ultrafiltration Membranes, Journal of Membrane Science, 108 (1995) 79-87.

[23] K. Boussu, Y. Zhang, J. Cocquyt, P. Van der Meeren, A. Volodin, C. Van Haesendonck, J.A. Martens, B. Van der Bruggen, Characterization of Polymeric Nanofiltration Membranes for Systematic Analysis of Membrane Performance, Journal of Membrane Science, 278 (2006) 418-427.

[24] T. Boccaccio, A. Bottino, G. Capannelli, P. Piaggio, Characterization of PVDF Membranes by Vibrational Spectroscopy, Journal of Membrane Science, 210 (2002) 315-329.

[25] C.-C. Ho, A.L. Zydney, Effect of Membrane Morphology on the Initial Rate of Protein Fouling During Microfiltration, Journal of Membrane Science, 155 (1999) 261-275.

[26] C.-C. Ho, A.L. Zydney, Theoretical Analysis of the Effect of Membrane Morphology on Fouling during Microfiltration, Separation Science and Technology, 34 (1999) 2461-2483.

[27] J. Hermia, Constant Pressure Blocking Filtration Laws- Application to Power-law Non-newtonian Fluids, Transactions of the Institute of Chemical Engineers, 6 (1982) 183-187.

[28] W.R. Bowen, J.I. Calvo, A. Hernandez, Steps of Membrane Blocking in Flux Decline during Protein Microfiltration, Journal of Membrane Science, 101 (1995) 153-165.
[29] C.-C. Ho, A.L. Zydney, A Combined Pore Blockage and Cake Filtration Model for Protein Fouling during Microfiltration, Journal of Colloid and Interface Science, 232 (2000) 389-399.

[30] L. Palacio, C.-C. Ho, A.L. Zydney, Application of a Pore-Blockage- Cake-Filtration Model to Protein Fouling During Microfiltration, Biotechnology and Bioengineering, 79 (2002) 260-270.

[31] G. Bolton, D. LaCasse, R. Kuriyel, Combined Models of Membrane Fouling: Development and Application to Microfiltration and Ultrafiltration or Biological Fluids, Journal of Membrane Science, 277 (2006) 75-84.

[32] R. Ghosh, Z.F. Cui, Purification of Lysozyme Using Ultrafiltration, Biotechnology and Bioengineering, 68 (2000) 191-203.

[33] J.M. Moss, M.-P.I. Van Damme, W.H. Murphy, P.F. Stanton, P. Thomas, B.N. Preston, Purification, Characterization, and Biosynthesis of Bovine Cartilage Lysozyme Isoforms, Archives of Biochemistry and Biophysics, 339 (1997) 172-182.

[34] J.A. Huntington, P.E. Stein, Structure and Properties of Ovalbumin, Journal of Chromatography B, 756 (2001) 189-198.

[35] P.E. Stein, A.G.W. Leslie, J.T. Finch, R.W. Carrell, Crystal Structure of Uncleaved Ovalbumin at 1·95Å Resolution, Journal of Molecular Biology, 221 (1991) 941-959.

[36] S. Brownlow, J.H.M. Cabral, R. Cooper, D.R. Flower, S.J. Yewdall, I. Polikarpov, A.C.T. North, L. Sawyer, Bovine β-lactoglobulin at 1.8 Å Resolution- Still an Enigmatic Lipocalin, Structure, 5 (1997) 481-495.

[37] K.J. Howe, K.P Ishida, M.M. Clark, Use of ATR/FTIR Spectrometry to Study Fouling of Microfiltration Membranes by Natural Waters, Desalination, 147 (2002) 251-255.

[38] S. Cinta-Pinzaru, S. Cavalu, N. Leopold, R. Petry, W. Kiefer, Raman and Surface-enhanced Raman Spectroscopy of Tempyo Spin Labelled Ovalbumin, Journal of Molecular Structure, 565-566 (2001) 225-229.

[39] R. Ionov, A. Hedoux, Y. Guinet, P. Bordat, A. Lerbret, F. Affouard, D. Prevost, M. Descamps, Sugar Bioprotective Effects on Thermal Denaturation of Lysozyme: Insights from Raman Scattering Experiments and Molecular Dynamics Simulation, Journal of Non-Crystalline Solids, 352 (2006) 4430-4436.

[40] Matsumoto, Characteristics of Ovalbumin Gel Layer Formed on Ceramic Microfiltration, Journal of Chemical Engineering of Japan, 29 (1996) 933-938.

[41] I.H. Huisman, P. Prádanos, A. Hernández, The Effect of Protein-Protein and Protein-Membrane Interactions on Membrane Fouling in Ultrafiltration, Journal of Membrane Science, 179 (2000) 79-90.

[42] K.M. Persson, F. Capannelli, A. Bottino, G. Tragardh, Porosity and Protein Adsorption of Four Polymeric Microfiltration Membranes, Journal of Membrane Science, 76 (1993) 61-71.

[43] S. Belfer, R. Fainchtain, Y. Purinson, O. Kedem, Surface Characterization by FTIR-ATR Spectroscopy of Polyethersulfone Membranes- Unmodified, Modified and Protein Fouled, Journal of Membrane Science, 172 (2000) 113-124.

[44] G. Shanmugam, P.L. Polavarapu, Vibration Circular Dichroism of Protein Films, Journal of the American Chemical Society, 126 (2004) 10292-10295.

[45] V. Chen, Performance of Partially Permeable Microfiltration Membranes under Low Fouling Conditions, Journal of Membrane Science, 147 (1998) 265-278.

[46] C.-K. Yeom, K.-H. Lee, Pervaporation Separation of Water-Acetic Acid Mixtures through poly(vinyl alcohol) Membranes Crosslinked with Glutaraldehyde, Journal of Membrane Science, 109 (1996) 257-265.

[47] B. Alberts, D. Bray, K. Hopkin, A. Johnson, J. Lewis, M. Raff, K. Roberts, P. Walter, Essential Cell Biology, 2nd Ed., Garland Science, USA, 2004.

[48] J.I. Boye, A.A. Ismail, I. Alli, Effects of Physiochemical Factors on the Secondary Structure of β-lactoglobulin, Journal of Dairy Research, 63 (1996) 97-109.

[49] S.T. Kelly, A.L. Zydney, Mechanisms for BSA Fouling during Microfiltration, Journal of Membrane Science, 107 (1995) 115-127.
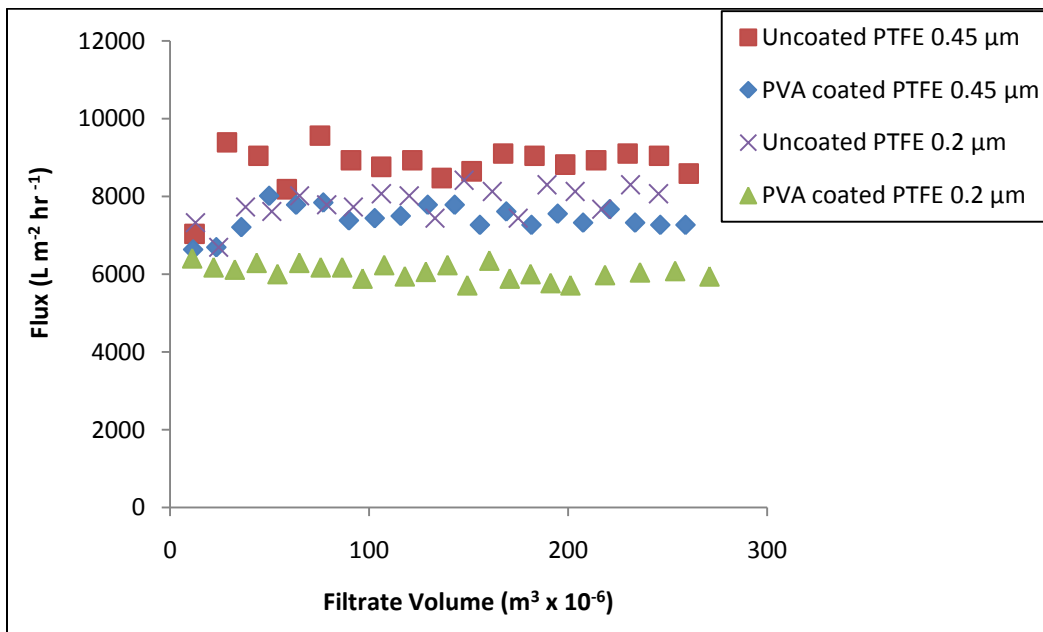
APPENDIX A

Figure 34: Permeate concentration versus filtrate volume determined by filtering through 0.45 μm uncoated or PVA PTFE membrane. Hemoglobulin solutions were prepared at isoelectric pH (7.2) and operated at 2 psi and 10 psi. The permeate concentration of the Hb was 2 g/L.

	Concentration before pre-filtration (g/L)	Concentration after pre-filtration (g/L)
Ovalbumin, uncoated PTFE, 2 g/L, 2 psi, 0.45 μm	2.079	1.996
Ovalbumin, uncoated PTFE, 2 g/L, 10 psi, 0.45 μm	2.074	1.982
Ovalbumin, PVA coated PTFE, 2 g/L, 10 psi, 0.45 μm	2.097	1.989
Ovalbumin, uncoated PTFE, 2 g/L, 10 psi, 1 μm	2.042	1.996
Ovalbumin, PVA coated PTFE, 2 g/L, 10 psi, 1 μm	2.031	1.997
β-lactoglobulin, PVA coated PTFE, 2 g/L, 10 psi, 0.45 μm	2.028	1.992
β-lactoglobulin, PVA coated PTFE, 2 g/L, 10 psi, 1 μm	2.020	1.958

Table 5: **Protein transmission before and after pre-filtration.**